

# **USE OF COUPLED NUMERICAL WAVE AND SURF MODELS TO SIMULATE THE LITTORAL ENVIRONMENT FROM DEEP WATER TO THE BEACH**

## **1.0 INTRODUCTION**

Development of numerical wave prediction models for purposes of wave forecasting and hindcasting has been a key part of wave research for several decades. Models generally address particular wave processes such as wave generation and propagation (in deep and/or shallow water), wave refraction/diffraction, or wave breaking. Each of these processes involves different physics, spatial scales, and numerical approaches. New types of amphibious systems and strategies require an integrated suite of models that provide predictive capability over a large region from deep water to the beach and along the coast. Several state-of-the-art models have been developed to the point that they can be implemented operationally or are already used operationally.

The Integrated Ocean Project (IOP) Program is identifying, linking, and operating a coupled suite of wave and surf models to provide automated calculations of wave conditions from deep water to and along the beach. Unlike traditional wave forecasting and hindcasting, this effort's goal is to develop a methodology so that wave conditions can be calculated realistically over large regions for simulations of military systems and amphibious operations. Outputs ultimately will be used as inputs to simulation and visualization software. The developed methodology accommodates replacement of particular models with updated or improved models as they become available. Models that are incorporated into IOP are the Regional Wave Model (WAM), ADvanced CIRCulation model (ADCIRC), STeady-State Spectral WAVE Model (STWAVE), REFraction/DIFfractiOn Model (REF/DIF1), and an updated version of the Navy Standard Surf Model (NSSM), SURF96. Model selection based on physics and practical implementation considerations, regions in which the models are most applicable, and model coupling techniques are described. Examples of coupled model output for Onslow Bay, NC, an important area for the military training and exercise community, are discussed. In addition, the IOP effort in support of the Synthetic Theater of War (STOW 97) Exercise is discussed.

The first section of this report pertains to the data needed for the models used in this research. These include wave spectra from WAM, wind forcing from the Navy Operational Regional Prediction System (NORAPS), and high-resolution bathymetry for Onslow Bay, NC. Section 3.0 presents an overview of the STWAVE model, a description of the modeling procedure, and Sec. 3.4 discusses sample results for Camp Lejeune. Section 4.1 describes an overview of the ADCIRC model, a description of the modeling procedure, and presents some sample results in Sec. 4.3. The REF/DIF1 model is described in Sec. 5.0, while Sec. 6.0 describes the SURF96 modeling procedure and discusses sample results for Camp Lejeune. Section 7.0 describes the IOP modeling effort that supported the STOW 97 Advanced Concept Technology Demonstration (ACTD). Sec. 8.0 describes the data sets discussed in this report that are available on-line through the Master Environmental Library (MEL). Finally, Sec. 9.0 summarizes this effort and provides model cautions and overall conclusions.

## 2.0 CAMP LEJEUNE MODELING EFFORT

### 2.1 Model Description

The IOP approach is to integrate a suite of physically consistent wave and surf models originating in deep water and progressing to shallow water into the surf zone. Figure 1 illustrates the IOP modeling procedure in which a regional WAM model can be coupled to the STWAVE and/or the REF/DIF1 shallow-water wave models. Tides from the ADCIRC model can be used by STWAVE, REF/DIF1, and NSSM. Outputs from STWAVE or REF/DIF1 can be used as inputs to NSSM. In this report, comparisons between STWAVE and REF/DIF1, as well as recommendations for their implementation, are made.

### 2.2 WAM

The WAM wave model is a spectral wave prediction model described by the WAMDI Group (1988; also Komen et al. 1994), an international consortium of wave modelers. WAM describes the sea surface as a discretized two-dimensional (2D) spectrum of sea surface elevation variance density. The Fleet Numerical Meteorology and Oceanography Command and Naval Oceanographic Office (NAVOCEANO) run operational global and regional implementations of WAM Cycle 4 (Wittmann and Farrar 1997). WAM used in this study is the Carolina regional WAM run by NAVOCEANO with a  $0.2^\circ$  resolution and spectra saved at selected locations. This Regional WAM is coupled to the  $1^\circ$  North Atlantic WAM. This implementation of the Regional WAM is not run routinely by NAVOCEANO. Rather, it is used for exercise support.

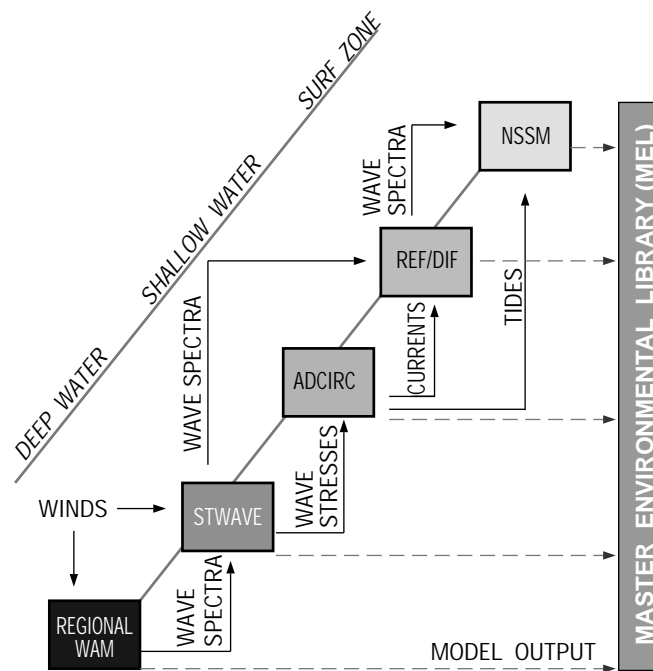


Fig. 1 — IOP modeling approach in which the deep-water WAM model is coupled independently to the STWAVE and REF/DIF1 shallow-water wave models; the outputs from one or both of these models are used as inputs into NSSM

WAM is discretized into 25 frequency bands with center frequencies ranging from 0.03333 to 0.32832 Hz, with each frequency being 1.1 times that of the next lower band. Direction is discretized into 24 bands of width  $15^\circ$ . WAM computes the wind-generated energy density of each spectral component. Energy is also propagated in space, with refraction due to depth variation and dispersion due to the nature of the waves. Because WAM spatial resolution does not resolve bathymetric variations close to a coast, WAM's refraction calculations apply to offshore regions rather than to the regions covered by STWAVE and REF/DIF1.

In this study, a 10-d period ranging from 12–22 Mar 1997 was selected in which WAM wave spectra were saved and subsequently used as inputs to the STWAVE and REF/DIF1 shallow-water wave models. Figure 2 shows the WAM domain and locations of the spectra used as inputs to STWAVE and REF/DIF1.

### 2.2.1 WAM Wind Forcing

The NORAPS for the Continental United States (CONUS) 10 m winds were used as inputs into the WAM (and STWAVE) hindcasts performed for the area including Onslow Bay, NC. CONUS NORAPS has a horizontal resolution of  $0.5^\circ$  and is run twice daily providing forecast products at 6-hourly intervals. The 12–22 Mar 1997 period was chosen to represent typical early spring conditions and included a storm event on 14 Mar producing waves in excess of 4 m as indicated by buoy observations and model results discussed in Sec. 2.2.2.

Figure 3 depicts comparisons between observed winds at buoy stations 41002, 41004, and CMAN station FPSN7 (see Fig. 2 for locations) and the NORAPS 10 m winds. Figure 3a–c shows good agreement with the wind direction for all three locations with buoy station 41002 showing the highest correlation ( $r = 0.92$ ) and CMAN station FPSN7, located at Frying Pan Shoals, with the lowest value of  $r = 0.82$ . The wind speeds in Fig. 3d–f show correlations ranging between 0.75 and 0.85, with root-mean-square (RMS) errors between 2.21 and 2.42 m/s. Winds on 12 Mar were from the northeast ahead of a warm front that passed to the north of the area by 9Z on 14 Mar. The winds gradually shifted from southerly ahead of an approaching cold front to the northwest on 15 Mar near 12Z. Winds were strongest at CMAN station FPSN7 on 14 Mar 18Z with a speed of 20 m/s. The

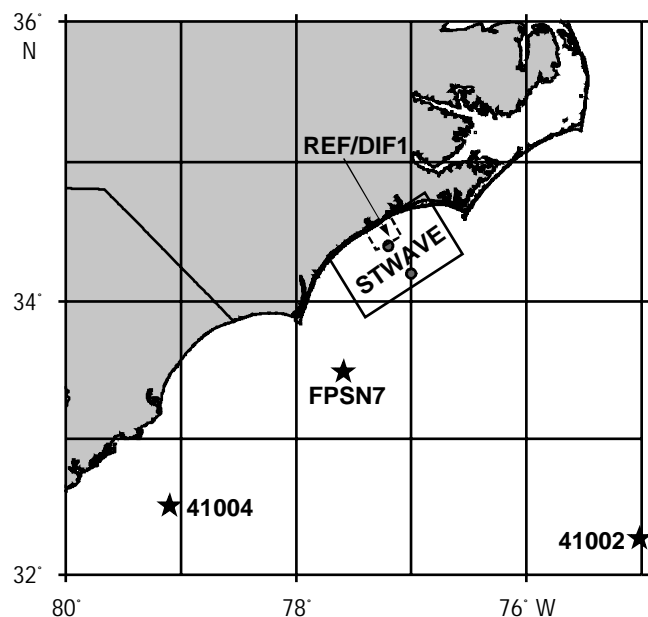


Fig. 2 — WAM domain for Carolina coastal area. Buoy stations (41002 and 41004) and CMAN station FPSN7 locations shown are used for model comparison. Also shown are the STWAVE and REF/DIF1 model areas.

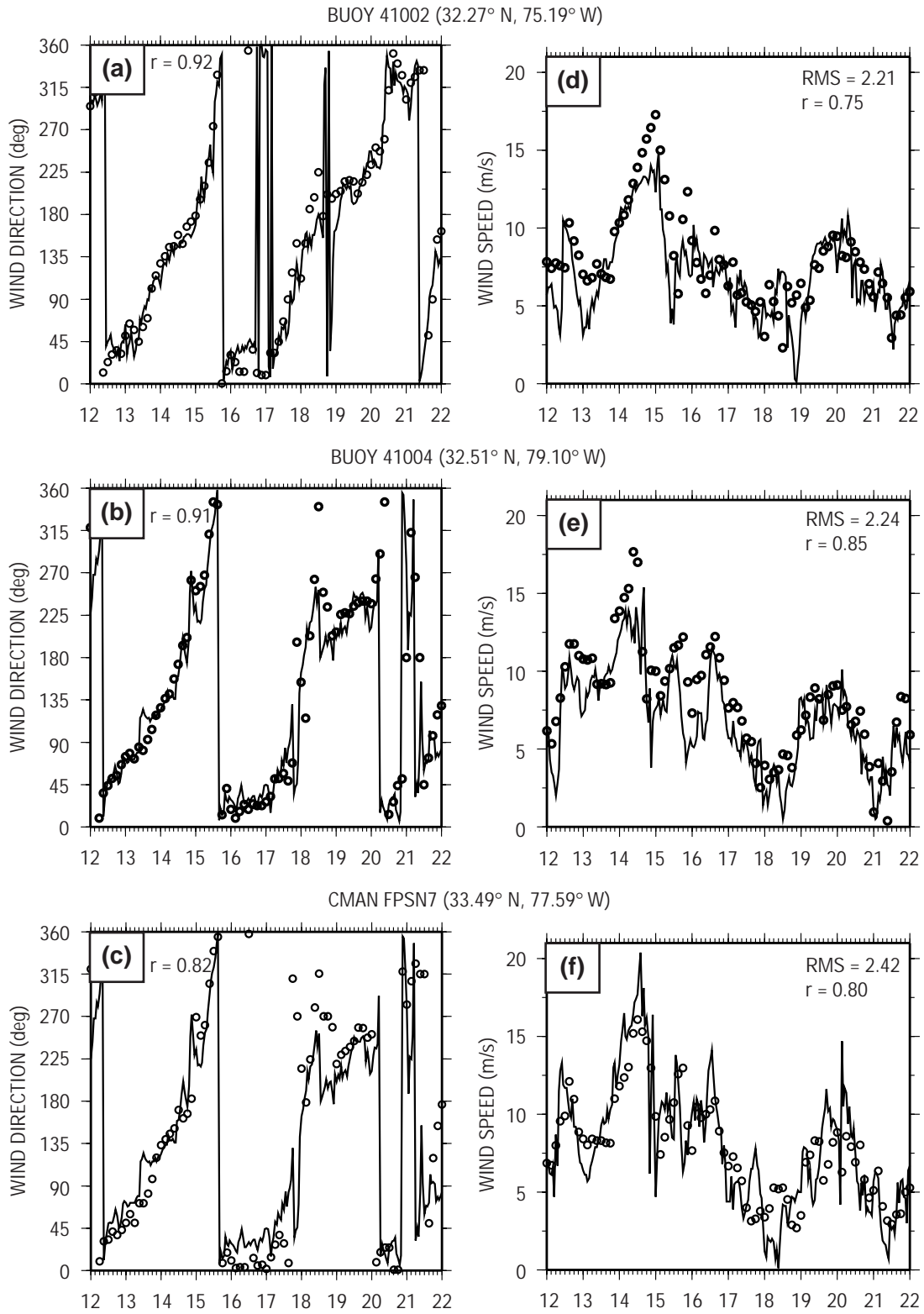


Fig. 3 — NORAPS (open circles) vs. buoy 41002, 41004, and CMAN FPSN7 (solid lines) for (a–c) wind direction and (d–f) wind speed during 12–22 Mar 1997

correlations shown here are reasonable considering that in addition to analyzed fields available every 12 h, NORAPS 6-h forecasts were included.

### 2.2.2 WAM Results

Typical WAM frequency and directional energy distributions from March 1997 are shown in Fig. 4. Figure 4a,b shows the peak of the storm on 14 Mar 18Z, with a peak wave period of 9.6 s and a mean wave direction of  $345^\circ$  (relative to north). At the peak of the storm, the winds that are generating the waves are over 18 m/s from the southeast and south (see Fig. 3). Figure 4c,d shows the frequency and directional energy distribution 24 h after the storm peak (15 Mar 18Z). The spectral peak from the storm is visible at a frequency of 0.1 Hz and a direction of  $330^\circ$ , but a second spectral peak around 0.17 Hz with a direction of  $180^\circ$  also appears. This second peak corresponds to a wind event with a wind speed of 15 m/s from the north (see Fig. 3). Figure 5 depicts contours of significant wave height (m) for the entire WAM model domain on 14 Mar 18Z. Maximum heights are found in the central portion of the area with values near 4.5 m. Arrows show the direction the waves are moving, generally from the south-southeast.

Figure 6a–c depicts comparisons of observed (solid line) versus WAM (open circles) significant wave height at buoy stations 41002 and 41004 and CMAN station FPSN7. The closest WAM gridpoint to the buoy was chosen as the comparison location. The maximum distance between a buoy location and model gridpoint was 17 km. Buoy station 41002, near the southeast corner of the model boundary, had the lowest correlation at 0.90 and an RMS error of 0.42 m. CMAN station

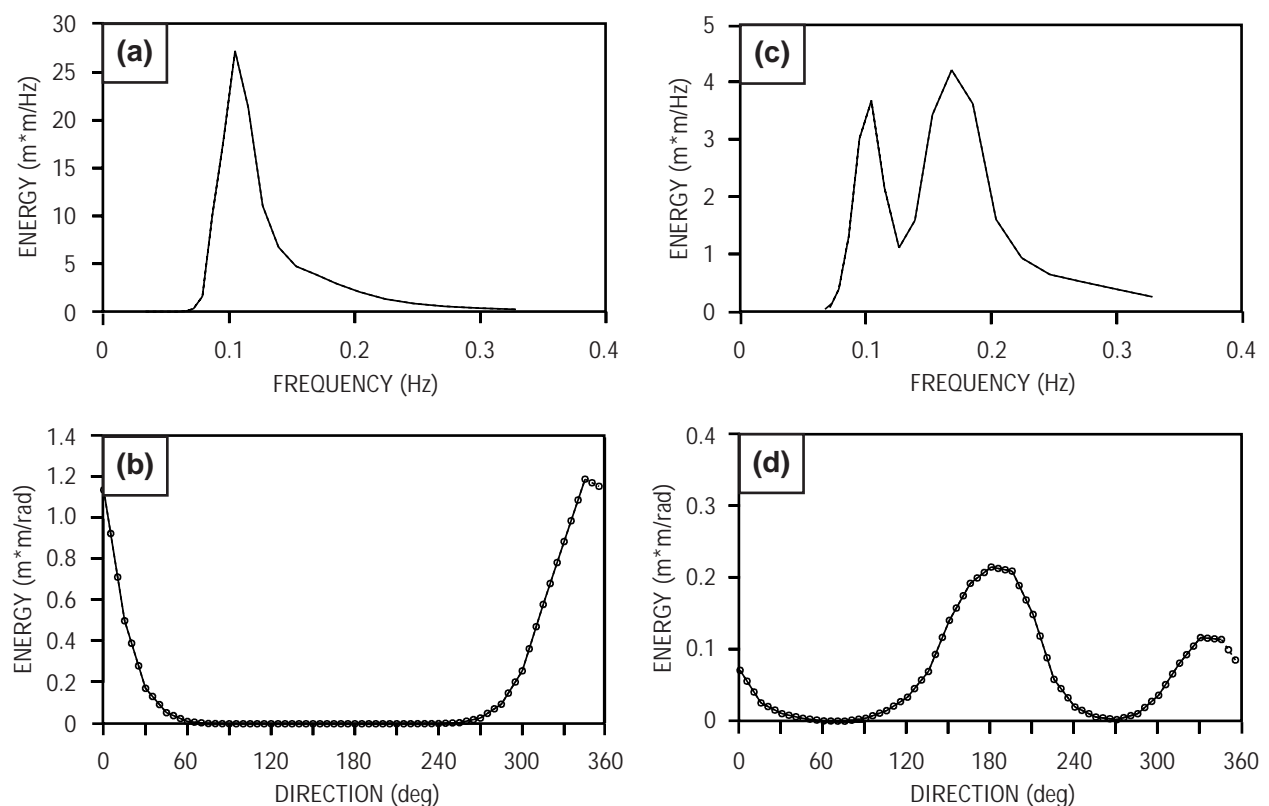


Fig. 4 — (a) WAM frequency and (b) directional distributions of wave energy for 14 Mar 1997 18Z. (c) WAM frequency and (d) directional distributions of wave energy for 15 Mar 1997 18Z.

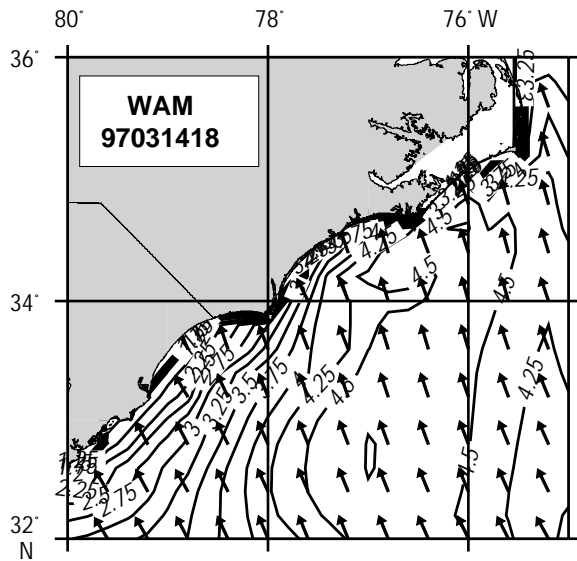


Fig. 5 — WAM significant wave height (m) for 14 Mar 1997 18Z. Arrows show direction waves are propagating.

FPSN7, closest to the STWAVE model grid, showed the highest correlation with  $r = 0.94$  and an RMS error of 0.29 m. Although all three buoys are outside the area of interest for the shallow-water modeling effort, they demonstrate that the WAM spectra used as input to STWAVE and REF/DIF1 are reasonable.

Mean wave period from WAM versus observation is shown in Fig. 6d–f. Wave periods range from 4–10 s, with the longest periods found during the peak of the storm on 14 Mar. Buoy station 41004 and CMAN station FPSN7 show reasonable correlation; however, WAM data near 41002 are consistently 2 s longer than observation. This behavior may be a computational artifact because buoy station 41002 is near the southeast corner of the WAM boundary.

### 2.3 Bathymetry Used for Shallow-Water Wave Modeling

The high-resolution Onslow Bay, NC, bathymetry used in the STWAVE and REF/DIF1 modeling effort was created using a Triangular Irregular Network (TIN) model. The TIN model (ESRI 1992) has the ability to incorporate a vector shoreline or a polygon as a breakline with a Z value to delineate land areas. The breakline is given a value (usually 0) and the areas between it and the nearest source data values are interpolated. The TIN model also handles irregularly spaced  $xyz$  locations and is typically used to represent terrain.

Three data sources were used to create the Onslow Bay bathymetry: (1) National Ocean Service (NOS) data, (2) Naval Research Laboratory (NRL) survey data, and (3) digitized data from a NAVOCEANO Special Tactical Oceanographic Information Chart (STOIC). Locations of raw hydrographic NOS data, shown in Fig. 7a, indicate that resolution is not adequate nearshore. Figure 7b shows the resultant bathymetry using NOS as the sole data source. Note the unrealistic isobaths near the coastline due to extrapolation. The NOS data were augmented with a high-resolution hydrographic survey collected by NRL Code 7242 on 18 Apr 1996 in support of the Joint Task Force Exercise Purple Star-96 (Nichols and Earle 1996). Improvement is evident in Fig. 7c; however, outside the domain of the high-resolution NRL survey data, the isobaths are still unrealistic nearshore. The final merged bathymetric product for Onslow Bay, shown in Fig. 7d, is based on a combination of NOS, NRL survey data, and data from a NAVOCEANO STOIC. The entire Onslow Bay bathymetry is shown in Fig. 7e.

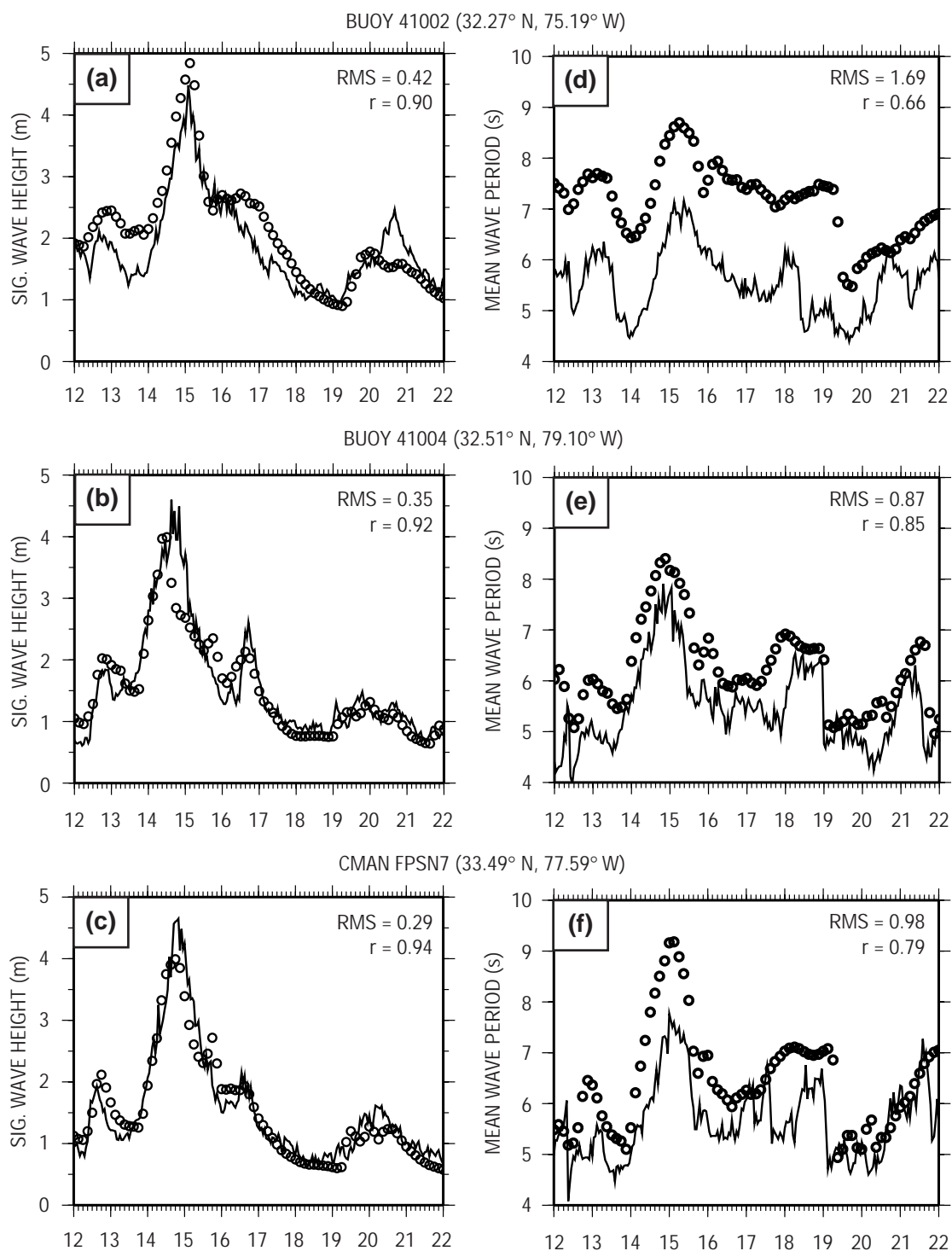


Fig. 6 — WAM (open circles) vs. buoy 41002, 41004, and CMAN FPSN7 (solid lines) for (a–c) significant wave height (m) and (d–f) mean wave period (s) during 12–22 Mar 1997

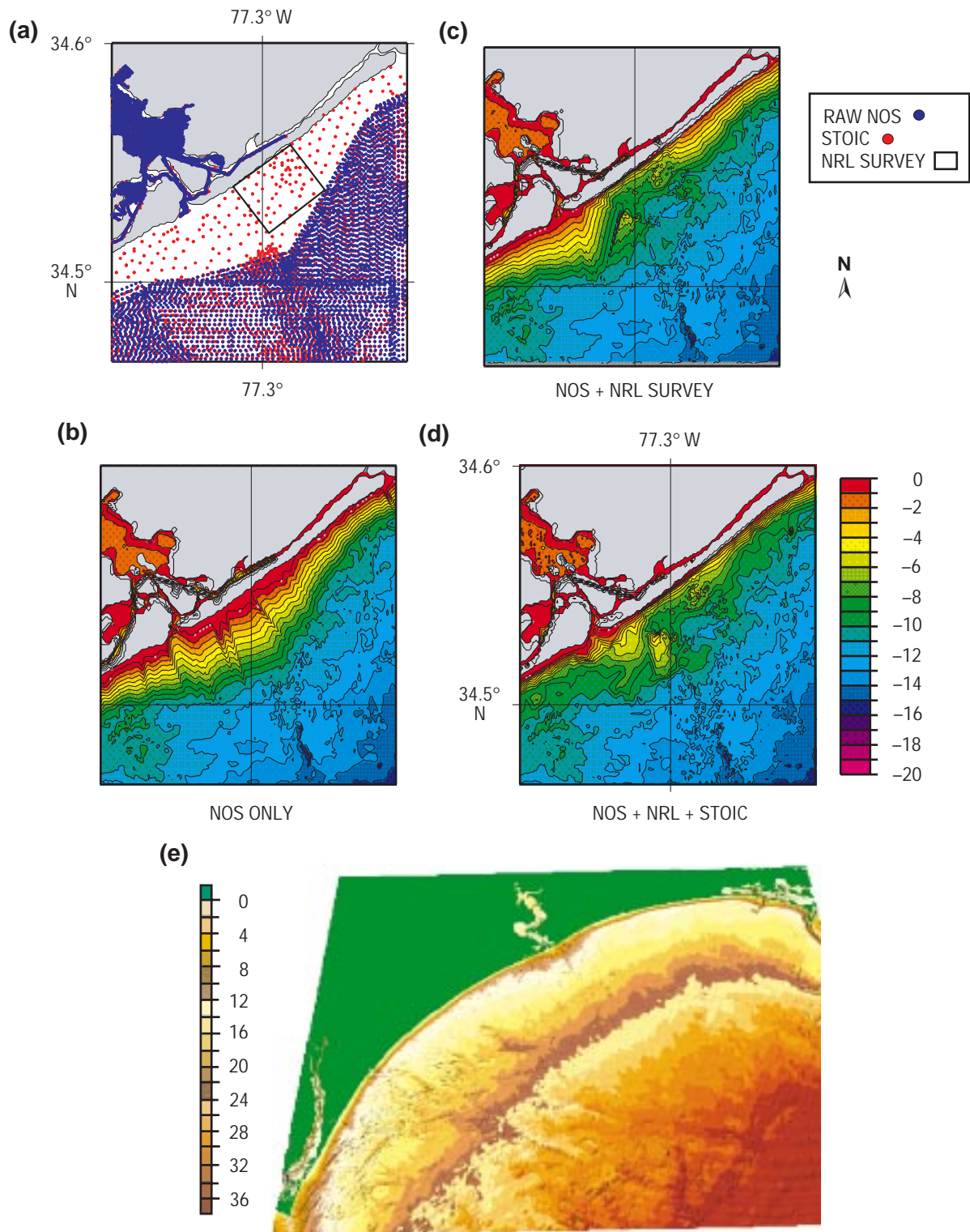


Fig. 7 — Generation of a high-resolution bathymetry for Onslow Bay, NC. (a) Locations of data sources, (b) resulting bathymetry (after running TIN model) using NOS only, (c) same as (b) but using NOS + NRL survey data, (d) combination of three data sources, and (e) final bathymetry for entire region.

### 3.0 STWAVE

#### 3.1 STWAVE Introduction

Nearshore waves and circulation were modeled for the period 12–23 Mar 1997 at Camp Lejeune, NC. The spectral wave transformation model STWAVE (Resio 1987, 1988a, 1988b; Davis 1992) was selected to transform offshore wave spectra that were hindcast using the WAM model (see Sec. 2.0) into the nearshore and surf zone. A spectral wave model was selected because it provides not only the wave height, period, and direction in the nearshore, but also 2D wave spectra (wave energy as a function of frequency and direction) to drive the surf model. The 2D spectra can be used to construct realistic water surface representations for environmental simulations.

#### 3.2 STWAVE Overview

The STWAVE model numerically solves the steady-state spectral energy balance equation:

$$\frac{\partial C_{g_x} E(f, \theta)}{\partial x} + \frac{\partial C_{g_y} E(f, \theta)}{\partial y} = \Sigma S, \quad (1)$$

where  $E$  = spectral energy density,  $f$  = frequency of spectral component,  $\theta$  = propagation direction of spectral component,  $C_g$  = group velocity of spectral component,  $x, y$  = spatial coordinates, and  $S$  = energy source/sink terms. The source terms include wind input, nonlinear wave-wave interactions, dissipation within the wave field, and surf-zone breaking. The terms on the left side of Eq. (1) represent wave propagation (refraction and shoaling) and the source terms on the right side of the equation represent energy growth or decay in the spectrum. The assumptions made in STWAVE are:

- mild bottom slopes,
- negligible wave reflection,
- spatially homogeneous offshore wave conditions,
- steady wave and wind conditions, and
- linear refraction and shoaling.

STWAVE is a half-plane model, meaning that waves only propagate toward the coast. Waves reflected from the coast or waves generated by winds blowing offshore are neglected. Surf-zone wave breaking limits the total wave height based on the local water depth.

STWAVE is a finite-difference model and calculates the wave spectra on a rectangular grid with square grid cells. The inputs required to execute STWAVE are:

- bathymetry and shoreline position,
- size and resolution of the grid,
- 2D wave spectrum on the offshore grid boundary, and
- wind speed and direction.

The model outputs zero-moment wave height ( $H_{m0}$ ), peak spectral period ( $T_p$ ), and mean wave direction ( $\theta_m$ ) at all gridpoints and the 2D spectrum at selected gridpoints.

### 3.3 STWAVE Modeling Procedure for Camp Lejeune

The wave modeling procedure is presented to document how simulations were performed for Camp Lejeune and to document the procedure for future applications. The modeling procedure includes generation of the finite-difference grid, specification of model input parameters, waves, winds, and model execution.

#### 3.3.1 Grid Generation

STWAVE operates on a flat grid with square grid cells. The optimal grid orientation is for the  $y$  axis to be aligned with the bathymetry contours and the  $x$  axis to be aligned normal to the contours. This orientation allows the greatest range of offshore wave angles and the most reliable modeling results. Bathymetry was supplied by NRL (see Sec. 2.3) for the Camp Lejeune region for latitudes from  $34.000^\circ$  to  $34.794^\circ$  N and longitudes from  $76.66^\circ$  to  $77.7^\circ$  W. The resolution was approximately 100 m. The STWAVE grid was generated using the ACES2.0 URGG (Uniform Rectilinear Grid Graphical User Interface) software (Leenknecht and Tanner 1997). Using URGG, the digital bathymetry file (in the format of  $x$ ,  $y$ , and  $z$ , with  $x$  and  $y$  in geographic coordinates and  $z$  in meters) were imported and the coordinates were transformed into Universal Transverse Mercator coordinates. The orientation of the grid was selected to be  $330^\circ$  relative to north, so the grid was aligned with the shoreline and bottom contours. The four corners of the grid are located at ( $34.756^\circ$  N,  $76.941^\circ$  W), ( $34.370^\circ$  N,  $76.660^\circ$  W), ( $34.020^\circ$  N,  $77.357^\circ$  W), and ( $34.405^\circ$  N,  $77.639^\circ$  W). For Camp Lejeune, the grid was specified as 201 cells in the cross-shore and 301 cells in the longshore with a grid resolution of 250 m. URGG uses Delauney triangulation to develop the grid and linear interpolation to assign elevations at each cell. After generation of the grid, the seabed elevations ( $-$  values) were converted to depths ( $+$  values) as required for STWAVE input.

#### 3.3.2 STWAVE Input

STWAVE input includes an options file that specifies the grid, use of the wind source term, spectral resolution, and model output locations. Two additional input files containing the water depths for the grid and the input spectra are required to run STWAVE.

**Options File.** A sample options file used for Camp Lejeune is given in App. A. The first line of the options file specifies the grid size (201 cross-shore and 301 longshore grid cells), the resolution of the 2D spectra (25 frequency and 35 direction bands), the grid resolution (250 m), two binary switches for including the wind source (0 = include winds) and nondimensionalizing the spectra (0 = not nondimensionalizing), and the number of output points for which spectra will be saved (14). Local wind forcing was used for the Camp Lejeune runs. The 35 spectral direction bands correspond to a  $5^\circ$  directional resolution. The next three lines in the sample options file are the central frequencies for the 25 frequency bins. These frequencies were selected to match the WAM output spectra used to drive STWAVE. The remaining lines of the options file identify the  $i$  (cross-shore) and  $j$  (along-shore) indices of the STWAVE output points where spectra are saved. The  $i = 1$  and  $j = 1$  gridpoint is in the northeast corner of the grid.

**Depth File.** The depth file contains the depths for each gridpoint. This file was generated using the procedure described under grid generation.

**Spectral Input File.** The main driver for the nearshore waves is wave spectra input on the offshore boundary of the STWAVE grid. These input spectra are the output from time-dependent WAM wave model runs, as discussed in Sec. 2.2.2. STWAVE is run with the same frequency

resolution as WAM. But, the STWAVE grid orientation and directional resolution differ from the WAM output. A  $0^\circ$  wave direction in WAM is a wave propagating to the north. In STWAVE, a  $0^\circ$  wave direction is propagating normal to the offshore edge of the grid. Thus, the WAM spectra were translated into the STWAVE orientation (STWAVE directions =  $330^\circ - \text{WAM directions}$ ). Also, the directional coverage and resolution differ between the WAM output and the STWAVE input. WAM spectra cover a full  $360^\circ$  with a resolution of  $15^\circ$ . STWAVE spectra cover a half plane ( $180^\circ$ ) with a resolution of  $5^\circ$ . WAM spectra were truncated to a half plane (neglecting waves traveling away from the coast) and the resolution was linearly interpolated from  $15^\circ$  to  $5^\circ$ . Figure 8 shows the WAM wave heights at the offshore boundary of the STWAVE grid ( $34.0^\circ$  N and  $77.0^\circ$  W) and the wave heights derived from the half-plane spectra used as the STWAVE boundary conditions. At times when the waves hindcast from WAM are moving toward the shore ( $240^\circ$  to  $60^\circ$ ), the WAM and STWAVE wave heights agree (e.g., on 14 Mar). When significant energy in the WAM hindcast is propagating offshore, the WAM wave energy exceeds the energy put into STWAVE, because the offshore propagating wave energy is neglected in STWAVE.

Wind speed and direction are also input to STWAVE in the spectral input file. The wind parameters were supplied from NORAPS (see discussion in Sec. 2.2.1). The NORAPS wind speed and direction at the STWAVE grid offshore boundary ( $34.2^\circ$  N and  $77.0^\circ$  W) are shown in Fig. 9. The wind direction, like the wave direction, was translated into the STWAVE reference frame for input to STWAVE. The wind speed and direction were assumed constant over the STWAVE model boundary.

### 3.3.3 STWAVE Execution

The wave and wind input to STWAVE come from time-dependent models. These models include temporal and spatial variations of the wave and wind fields over large spatial domains. Since the nearshore region of interest at Camp Lejeune is relatively small, the time variation of the waves is modeled with a series of steady-state simulations. STWAVE was run at 3-h increments for the time period 12 Mar 03Z to 23 Mar 1997 at 00Z. A total of 88 model runs were made. A steady-state wave model is much more computationally efficient than a time-dependent model for the fine grid resolution required in the nearshore. Depth changes due to the tide and wind, calculated from ADCIRC, were included in these simulations.

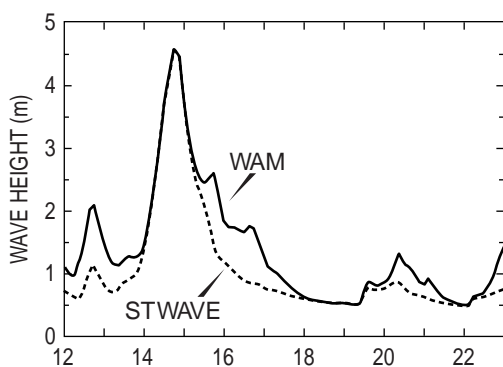


Fig. 8 — WAM output and STWAVE input wave heights for 12–23 Mar 1997 ( $34.2^\circ$  N,  $77.0^\circ$  W)

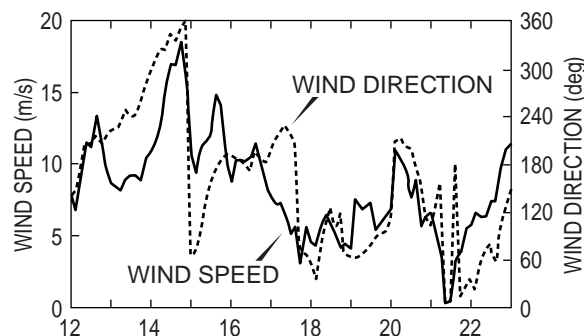


Fig. 9 — NORAPS wind speed and direction for 12–23 Mar 1997 ( $34.2^\circ$  N,  $77.0^\circ$  W)

The model output includes the wave height (meters), peak period (seconds), and mean direction (degrees relative to the STWAVE grid) for all gridpoints and the wave spectra ( $\text{m}^2/\text{Hz}/\text{rad}$ ) for selected locations. STWAVE was executed on a Digital Equipment Company Alpha workstation at the U.S. Army Corps of Engineers Waterways Experiment Station. The spectra were saved for 14 gridpoints for each model run. The output spectra for these locations were used as input to other models and ingested into MEL for easy access by the modeling and simulation community.

### 3.4 Camp Lejeune STWAVE Sample Results

The previous section discussed the procedure used to apply STWAVE to calculate nearshore wave spectra at Camp Lejeune. This section shows sample results.

Figure 10 shows the depth contours over the STWAVE grid. The contours are in meters, with 0 m representing the shoreline. Contour lines are drawn at 5-m intervals. The foreshore slope is relatively steep out to a depth of 10 m where it becomes very gentle. The contours are approximately parallel to the shoreline. The offshore edge of the grid is at a depth of 30 m. Since the bathymetry at Camp Lejeune is quite regular (approximately straight-parallel contours), the wave transformation is fairly uniform along the shore. The dominant processes are wave shoaling, refraction, and surf-zone breaking. Because of its grid resolution, STWAVE does not adequately resolve the surf zone which is modeled by NSSM.

Figure 11 shows transformed frequency and directional distributions of wave energy at four locations on the STWAVE grid (14 Mar 1997 at 18Z). The locations represent a cross-shore transect at the central section of the beach. The local water depths for Fig. 11 are 25.3, 6.5, 4.1, and 1.6 m, respectively. The wave directions are relative to the STWAVE grid, so  $0^\circ$  is a wave propagating toward  $330^\circ$  relative to north, positive angles are more toward the west and south, and negative angles are more toward the north and east. The shape of the frequency spectra stays about constant for each location, but the energy level decreases due to wave breaking. The spectral shape stays constant because there is little or no additional wave growth between locations. The directional

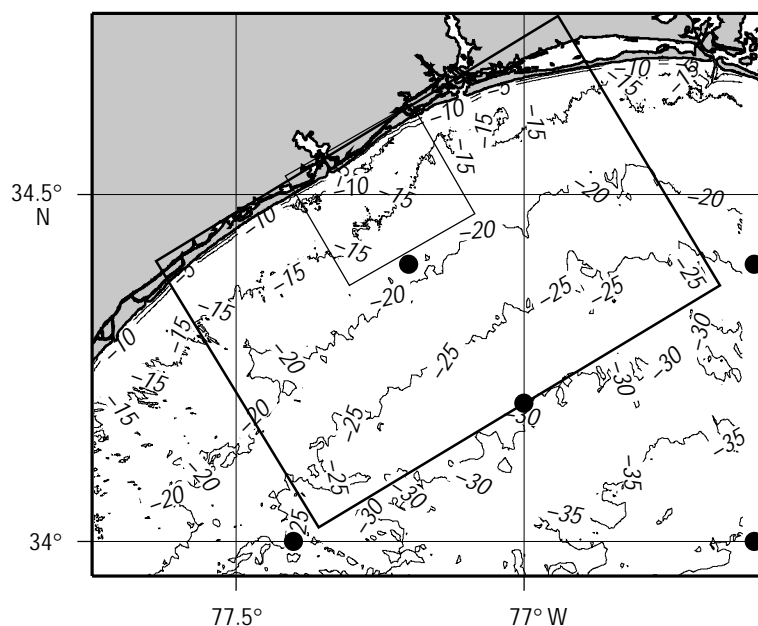


Fig. 10 — Camp Lejeune bathymetry used in STWAVE grid. Circles denote locations of available WAM spectra. Small rectangle embedded within STWAVE grid is REF/DIF1 domain.

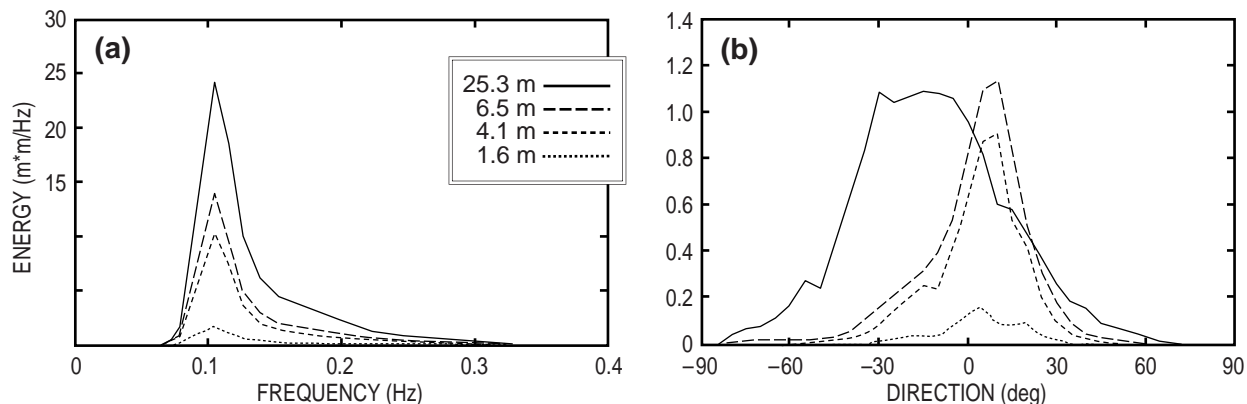


Fig. 11 — STWAVE wave spectrum for 14 Mar 1997 at depths of 25.3, 6.5, 4.1, and 1.6 m

distribution of energy becomes narrower and more peaked in shallow depths. This is due to refraction turning the waves so they are more shore normal.

Figure 12 shows contours of wave height for the same time period. The wave height shoals slightly between the 4.5 and 4 m contours and then decays due to whitecapping. Very nearshore, the wave height decays due to depth-limited breaking.

Wind speed and direction impact wave transformation. The wind speeds at Camp Lejeune were significant (exceeding 18 m/s) during the simulation periods. The wind has two impacts on the nearshore waves, turning of the wave direction and, at some times, further growth or decay of the waves.

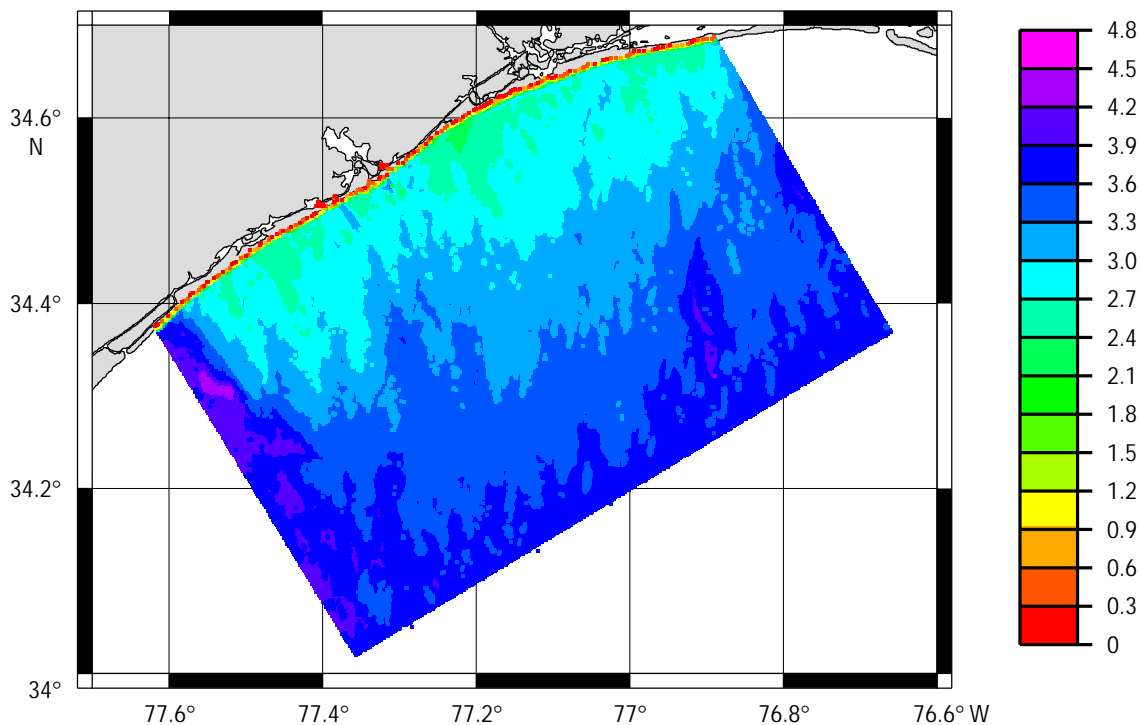


Fig. 12 — STWAVE wave height contours (m) on 14 Mar 1997 18Z

## 4.0 ADCIRC

The hydrodynamic model ADCIRC-2DDI (Luettich et al. 1992, Westerink et al. 1994) was selected to calculate water surface elevations and currents in the nearshore. The water elevations serve as input conditions for nearshore wave models. This 2D, finite-element model uses tidal constituents, wind, and atmospheric pressure as input and outputs water surface elevations and currents.

### 4.1 ADCIRC Overview

The ADCIRC model is based on the Generalized Wave-Continuity Equation (GWCE) formulation of the depth-integrated continuity and momentum equations (Lynch and Gray 1979, Luettich et al. 1992). The GWCE in Cartesian coordinates is given by

$$\begin{aligned} \frac{\partial^2 \zeta}{\partial t^2} + \tau_0 \frac{\partial \zeta}{\partial t} + \frac{\partial}{\partial x} \left( U \frac{\partial \zeta}{\partial t} - UH \frac{\partial U}{\partial x} - VH \frac{\partial U}{\partial y} + fVH - H \frac{\partial}{\partial x} \left[ \frac{p_s}{\rho_0} + g(\zeta - \alpha\eta) \right] \right. \\ \left. - E_{h2} \frac{\partial^2 \zeta}{\partial x \partial t} + \frac{\tau_{sx}}{\rho_0} - (\tau^* - \tau_0)UH \right) + \frac{\partial}{\partial y} \left( V \frac{\partial \zeta}{\partial t} - UH \frac{\partial V}{\partial x} - VH \frac{\partial V}{\partial y} + fUH - H \frac{\partial}{\partial y} \right. \\ \left. \left[ \frac{p_s}{\rho_0} + g(\zeta - \alpha\eta) \right] - E_{h2} \frac{\partial^2 \zeta}{\partial y \partial t} + \frac{\tau_{sy}}{\rho_0} - (\tau^* - \tau_0)VH \right) = 0, \end{aligned} \quad (2)$$

where  $E_{h2}$  = horizontal eddy diffusion/dispersion coefficient,  $f$  = Coriolis parameter,  $g$  = gravitational acceleration,  $H$  = total water depth ( $\delta + h$ ),  $h$  = bathymetric depth relative to a datum,  $P_s$  = atmospheric pressure at the free surface,  $t$  = time,  $U$ ,  $V$  = depth-averaged horizontal velocities,  $\alpha$  = effective Earth elasticity factor,  $\eta$  = Newtonian equilibrium tide potential,  $\rho_0$  = density of water,  $\tau_{sx}$ ,  $\tau_{sy}$  = free surface stresses,  $\tau^* = C_f (U^2 + V^2)^{1/2}/H$ ,  $C_f$  = bottom friction coefficient,  $\tau_0$  = constant, and  $\delta$  = free surface elevation relative to a datum.

In ADCIRC, the GWCE is solved together with the primitive form of the momentum equations

$$\frac{\partial U}{\partial t} + U \frac{\partial U}{\partial x} + V \frac{\partial U}{\partial y} - fV = - \frac{\partial}{\partial x} \left[ \frac{p_s}{\rho_0} + g(\zeta - \alpha\eta) \right] + \frac{1}{H} M_x + \frac{\tau_{sx}}{\rho_0 H} - \tau^* U \quad (3)$$

$$\frac{\partial V}{\partial t} + U \frac{\partial V}{\partial x} + V \frac{\partial V}{\partial y} - fU = - \frac{\partial}{\partial y} \left[ \frac{p_s}{\rho_0} + g(\zeta - \alpha\eta) \right] + \frac{1}{H} M_y + \frac{\tau_{sy}}{\rho_0 H} - \tau^* V, \quad (4)$$

also given in Cartesian coordinates, where  $M_x$  and  $M_y$  are depth-integrated horizontal diffusion/dispersion. The Camp Lejeune application was run in spherical coordinates. The forcing/resisting terms include Coriolis, tide potential, surface stress (winds), atmospheric pressure, and bottom

friction. Advection and diffusion/dispersion terms are also included. The assumptions made in ADCIRC are:

- incompressibility,
- hydrostatic pressure,
- neglect baroclinic terms,
- quadratic bottom stress formulation, and
- turbulent diffusion and momentum dispersion modeled with eddy viscosity model.

ADCIRC is a finite-element model and calculates the water surface elevation and current on an unstructured grid. The inputs required to execute ADCIRC are:

- bathymetry and shoreline position,
- specification of a finite-element grid and boundary conditions,
- tidal constituents along the grid boundary, and
- wind speed and direction and atmospheric pressure (if used).

The model outputs water surface elevation and current at selected gridpoints.

## 4.2 ADCIRC Modeling Procedure for Camp Lejeune

The modeling procedure for Camp Lejeune included generation of the finite-element grid, specification of model input parameters and winds, and model execution.

### 4.2.1 Grid Generation

The ADCIRC grid for the North Carolina coast, including Camp Lejeune, is shown in Fig. 13. The large extent of the grid provides more accurate simulations by moving the boundaries away from the coast of interest. The grid was generated using the ACE/gredit (**A**nalysis of **C**oasts and **E**stuaries grid editor) software (Turner and Baptista 1993). Bathymetry used to generate the grid came from NOS and Navy data bases. The grid resolution is approximately 0.5 km at Camp Lejeune with higher resolution near the coastal inlets.

Wind speed and direction are also input to ADCIRC. The wind parameters were supplied from NORAPS at a 0.5° resolution. M2 semidiurnal tidal constituents of amplitude and phase input along the grid boundary were supplied from the Dredging Research Program tidal constituent data base (Westerink et al. 1993).

### 4.2.2 ADCIRC Input

ADCIRC input includes a grid file and an options file. Additional optional input files include a hot start file and a file containing the wind fields (and atmospheric pressure fields, if used).

**Grid File.** The grid file is generated by the ACE/gredit and contains the latitude, longitude, and depth for each gridpoint.

**Options File.** The options file specifies model parameters (e.g., time step, run time, bottom friction coefficients, output points). Appendix B is a truncated sample options file with short

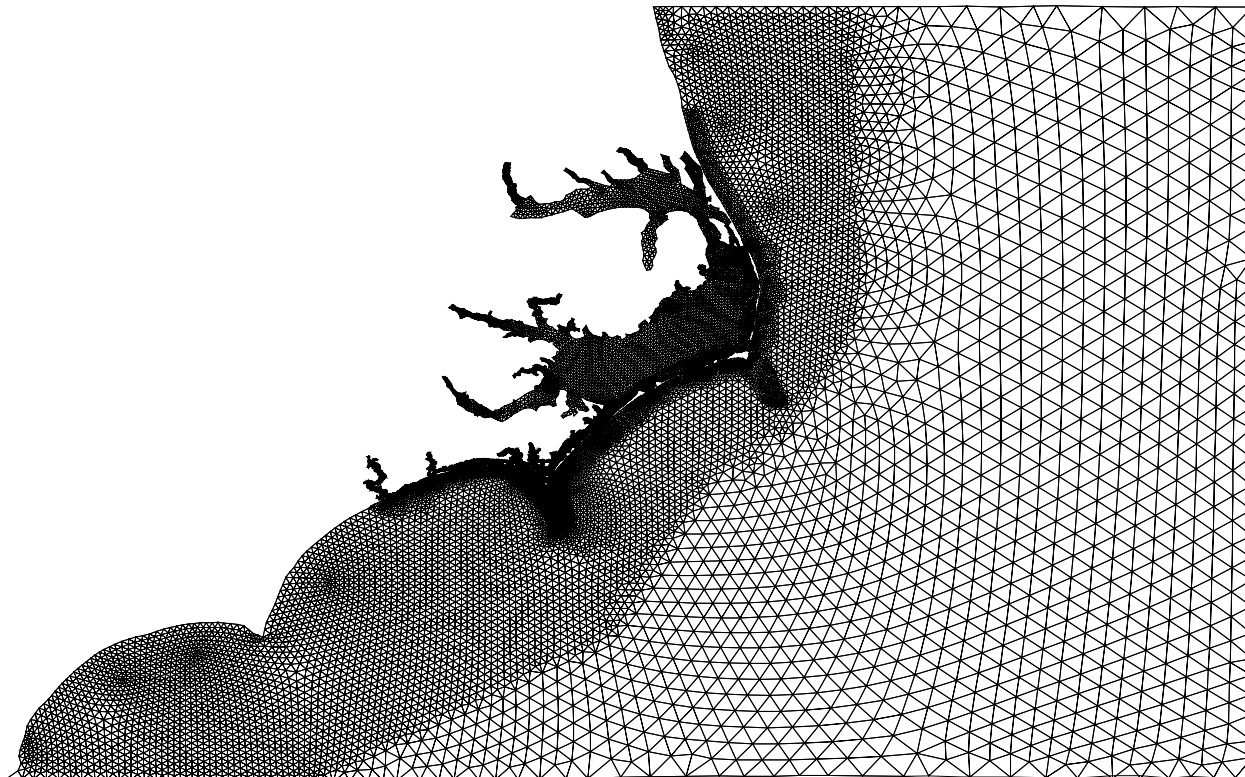


Fig. 13 — ADCIRC grid for Onslow Bay, NC region

explanations of parameters. ADCIRC was run for Camp Lejeune with a 4-s time step for 13 d in spherical coordinates (latitude–longitude). Depth nonlinearities were included, but advection terms were neglected. Bottom friction and viscosity were held constant, but a spatially variable wind field was applied. M2 tidal constituents were applied along the model open boundaries. Model velocities and elevations were saved at 15 locations within the domain (seven near Camp Lejeune and eight elsewhere in the domain). Detailed information on the options file is given by Westerink et al. (1994).

**Wind File.** The wind vectors from NORAPS were supplied as a separate input file.

**Hot Start File.** A hot start file containing velocities and elevations during a spin-up period prior to the simulation dates was also supplied as input.

#### 4.2.3 ADCIRC Execution

ADCIRC was ramped up over a 1-d period prior to 10 Mar 1997 and the resulting velocities and water levels were saved in a hot start file. These data were then used to jump-start the model on 10 Mar. An additional ramp-up period of 2 d prior to 12 Mar was used for a simulation length of 13 d. Output water surface elevations (m) and depth-integrated velocities (m/s) at 10-min intervals were saved at nearshore locations to feed into nearshore wave model simulations.

### 4.3 Camp Lejeune Sample ADCIRC Results

This section illustrates some sample results from the ADCIRC application at Camp Lejeune. ADCIRC results at two locations at Onslow Beach are presented: an offshore station ( $34.2^\circ$  N,  $77.0^\circ$  W) at a depth of 30 m and a nearshore station ( $34.53^\circ$  N,  $77.25^\circ$  W) at a depth of 12 m. The offshore station corresponds to the offshore boundary of the STWAVE grid, and elevation data from this station were used to specify the tide in the STWAVE runs.

Figures 14 and 15 show water surface elevations at offshore and nearshore stations, respectively. The M2 tidal range at Onslow Beach is a little less than 1 m (0.8 m at the offshore point and 0.9 m at the nearshore point). The phasing between the two stations shown in Figs. 14 and 15 is almost identical, which is expected since the locations are relatively close, but the water surface amplitudes are as much as 20 percent higher at the shallower location. The modulation of the water surface

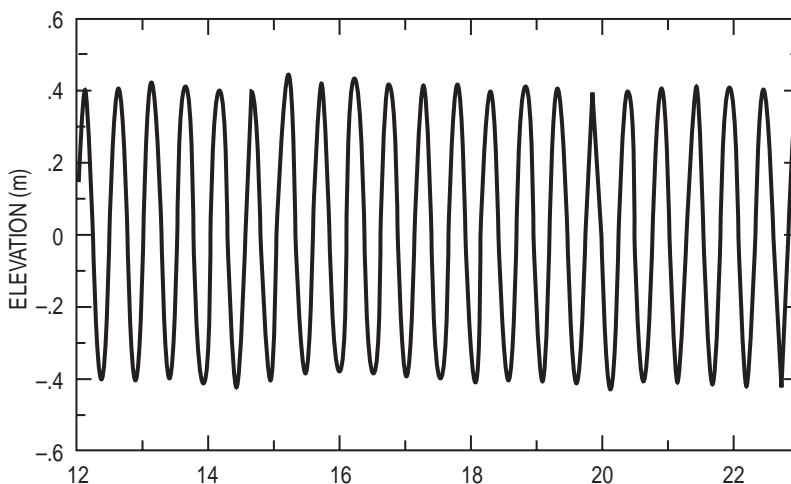


Fig. 14 — Water surface elevations for offshore point  $34.2^\circ$  N,  $77.0^\circ$  W for 12–22 Mar 1997

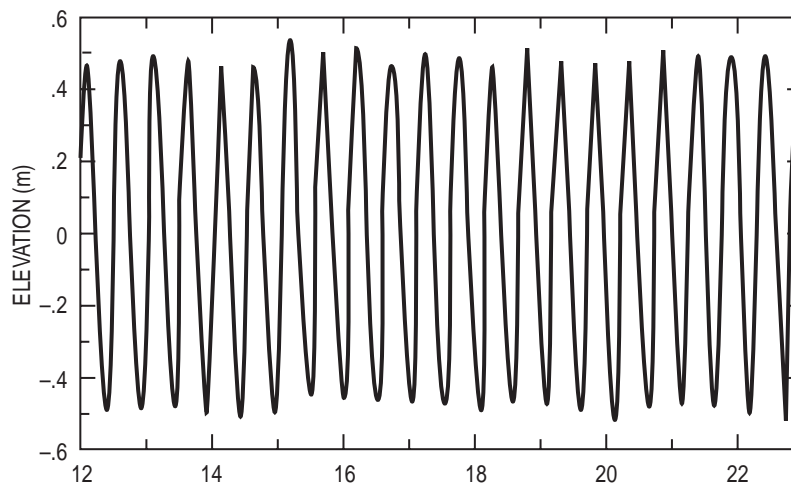


Fig. 15 — Water surface elevations for on-shore point  $34.53^\circ$  N,  $77.25^\circ$  W for 12–22 Mar 1997

signal shown in the plots is due to the wind, since only the dominant M2 tidal constituent was used. The wind effect is stronger at the nearshore station because of the shallower depth and closeness to the beach.

Figures 16 and 17 show ADCIRC velocities at the same stations shown in Figs. 14 and 15, respectively. The  $x$  velocity is the east-west component with positive velocities to the east and the  $y$  velocity is the north-south component with positive velocities to the north. At both locations at Onslow Beach, the peak velocities occur near a zero tide level, with predominant flow to the west of a rising tide and to the east of a falling tide. The north-south velocity component is about 50 percent of the east-west component at the nearshore station, and the flow is to the east-northeast on falling tides and to the west-southwest on rising tides. At the offshore station, the north-south velocity component is only 15 percent of the east-west flow, and the flow is slightly south of east of falling tides and north of west of rising tides. The difference in phases of the north-south velocities between the two stations is possibly due to their differences in position relative to the New River Inlet or other nearby inlets. The wind modulates the velocities in a manner similar to

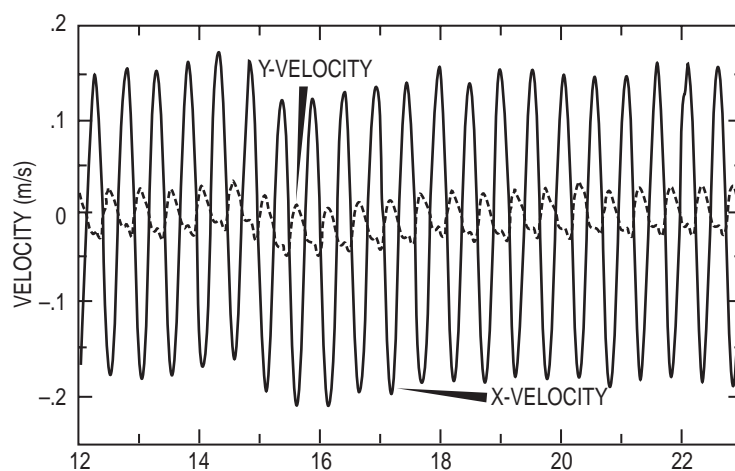


Fig. 16 — Velocities for offshore point  $34.2^{\circ}$  N,  $77.0^{\circ}$  W for 12–22 Mar 1997

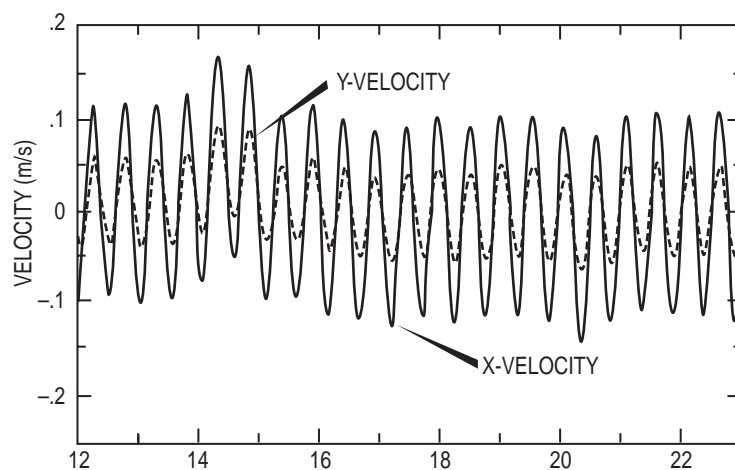


Fig. 17 — Velocities for nearshore point  $34.53^{\circ}$  N,  $77.25^{\circ}$  W for 12–22 Mar 1997

the water elevations causing stronger onshore flows during the onshore wind events (e.g., 14 Mar) and offshore flows during offshore wind events (e.g., 20 Mar).

## 5.0 REF/DIF1 INTRODUCTION

In shallow water, wave propagation is strongly affected by the underlying bathymetry and currents. The dynamic processes include shoaling, refraction, diffraction, wave-current interaction, and energy dissipation due to bottom friction and depth-induced breaking. The coastal wave model REF/DIF1 was developed to model these processes (Kirby and Dalrymple 1994). REF/DIF1 is chosen to simulate waves in shallow water because of its rigorous treatment of combined refraction and diffraction process.

### 5.1 REF/DIF1 Overview

The REF/DIF1 model solves the mild slope equation with the parabolic approximation. Berkhoff's mild slope equation written in terms of surface displacement,  $\eta(x,y)$ , and horizontal gradient operator is

$$\nabla_h \cdot (CC_g \nabla_h \eta) + \sigma^2 \frac{C_g}{C} \eta = 0 . \quad (5)$$

Here,

$$C = \sqrt{g/k} \tanh kh, \text{ the phase velocity}$$

$$C_g = C (1 + 2kh/\sinh 2kh)/2, \text{ the group velocity,}$$

where the local water depth is  $h(x,y)$  and  $g$  is the acceleration of gravity. The local wavenumber,  $k(x,y)$ , is related to the angular frequency of the waves,  $\sigma$ , by the linear dispersion relationship  $\sigma^2 = gk \tanh(kh)$ .

Kirby and Dalrymple (1983) derived another form of the equation, bridging the gap between the nonlinear diffraction and the linear mild slope equation. The effect of wave-current interaction was treated by Kirby (1984). Kirby (1986a, 1986b) further developed the equation for a wide-angle parabolic approximation. Details of the final form of the equation and parabolic approximation approach can be found in Kirby's papers and in Kaihatu et al.'s review (1998) of REF/DIF1 and related models. The equation is solved in finite-difference form using a Crank-Nicolson implicit scheme.

The REF/DIF1 model is designed for simulation of monochromatic and unidirectional wave train propagation. For any realistic wave condition consisting of a various combination of wind, waves, and swell, the user needs to make independent REF/DIF1 runs for wave components at fine frequency and direction bandwidths. The results of these separate runs are linearly combined. Outside the surf zone where depth-induced breaking rarely occurs, the superposition approximation is valid and was successfully applied to the Southern California Bight by O'Reilly and Guza (1993).

Instead of running wave models each time for new input (a time-consuming process), a transfer function approach can be applied for wave hindcasts, nowcasts, or forecasts. In this approach, calculations are made for all possible frequency and angular components, and the results are saved in a tabular form. The user only needs to derive the transfer function (called transformation coefficients) once for a given area. The transfer function at any point in the model domain consists of amplitude and phase as functions of input wave frequency and angle. For any given wave spectrum input, the spectrum is first divided into many wave components. The amplitude and direction of individual wave components is modified by the corresponding transfer function and then linearly combined with the results from other components to derive the final results.

The assumptions made in REF/DIF1 are similar to STWAVE:

- mild bottom slopes,
- negligible wave reflection, and
- spatially homogeneous offshore wave conditions along the model's seaward grid edge.

## 5.2 REF/DIF1 Modeling Procedures

The modeling procedures include grid generation, specification of input parameters including input wave conditions, and generation of transfer coefficients.

### 5.2.1 Grid Generation

For the Camp Lejeune runs, the offshore boundary of the model grid is centered on the WAM output point at 34.4° N and 77.2° W. The 3-s Onslow Bay bathymetry described in Sec. 2.3 was used in REF/DIF1. The number of gridpoints are 180 and 250 in  $x$  (normal to the shore) and  $y$ , respectively. A grid rotation of 30° (same rotation angle used in STWAVE) was chosen so that the offshore depth contours are nearly parallel to the grid boundary. Figure 18 depicts the bathymetry and domain of the REF/DIF1 grid. The grid resolution was 92.5 m in both  $x$  and  $y$  axes, close to the original 100-m resolution bathymetry. Although Kirby's wide-angle approach to a parabolic model such as REF/DIF1 extends the valid input angle to  $\pm 70^\circ$ , results beyond an input angle of 50° are slightly degraded. It is often necessary to use more than one model grid with various rotations to cover the full range of possible angles. Since the offshore boundary in our case is rather shallow with a depth of 18.4 m, any other rotated grid will render one end of the grid much shallower than the other end. This will result in an inaccuracy in estimating the mean wavelength. Consequently, the increase in accuracy of using multiple rotated grids is limited and was not pursued in our simulations.

**Input Parameters.** The input parameters include wave frequency, angle, height, grid information, and tidal level. Other information with regard to selection of dissipation mechanisms and lateral boundary conditions are also specified.

**Grid Resolution.** REF/DIF1 automatically increases the grid resolution, i.e., subdividing the original grid in the  $x$  axis if necessary, as the wavelength gets shorter in shallow water. Phase-resolving wave models typically require at least 6 points per wavelength as a grid resolution to avoid spatial aliasing. REF/DIF1 does not provide automatic gridding in the  $y$  axis. Instead, a fixed parameter for subdivision in the  $y$  axis,  $nd$ , for the whole grid is a required user-selected input parameter. To avoid aliasing in the  $y$  axis, increasing values of  $nd$  were used as the wavelength gets shorter in these runs.

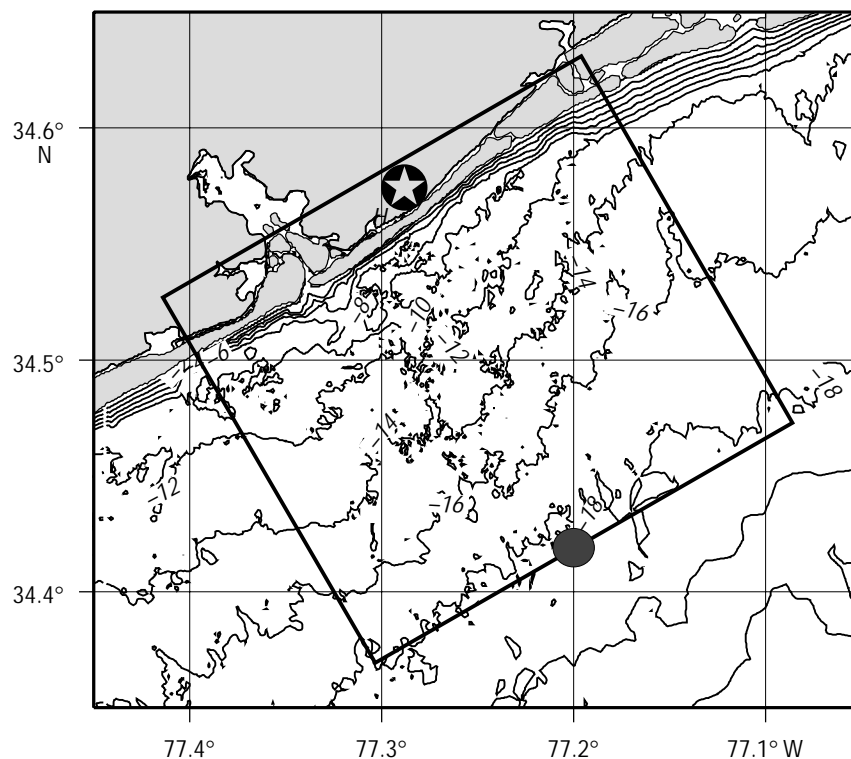


Fig. 18 — REF/DIF1 grid for Onslow Bay, NC. Circle on outer boundary indicates location of WAM deep-water spectra, which was used as a boundary condition. The star near the beach denotes the location of the landing beach.

**Run Bandwidths.** The resolution of frequency and directional bandwidths required for the transfer function depends on the bathymetry and wave climate. Discussions of bandwidth and other REF/DIF1 modeling issues are covered by Kaihatu et al. (1997). Evaluation runs were first conducted. The transfer functions are variable over a directional spread of a few degrees. Similar variations have been reported by O'Reilly and Guza (1993). Based on the evaluation runs, the model was run for  $2^\circ$  bandwidths ranging from  $-70$  to  $+70^\circ$  relative to the model grid, with 18 frequencies ranging from 0.06 to 0.35 Hz. From 0.06 to 0.20 Hz, model runs were conducted at 0.01 Hz intervals. For high-frequency waves above 0.20 Hz, the frequency interval increases to 0.50 Hz. All together, 1278 individual wave runs were conducted. A run script was written to perform repetitive runs.

**Miscellaneous.** Open lateral boundary conditions were specified to avoid reflection from the boundary. Since the tidal range is not large and output points start at a depth of 7 m, no tidal level was used for the Camp Lejeune runs. Due to the small model domain, the bottom dissipation option was not activated for this simulation.

### 5.3 Sample REF/DIF1 Results for Camp Lejeune

The transfer functions for selected locations at various depths ranging from 7–9 m were saved. The input WAM directional spectrum has a logarithmic frequency distribution whereas the REF/DIF1 runs are conducted at equal frequency intervals. To derive the final directional spectra, WAM spectra were first interpolated to REF/DIF1 frequencies before applying the transfer function. The evolution of sea state for 14 Mar (00–18Z) is illustrated in Fig. 19. The saturation of

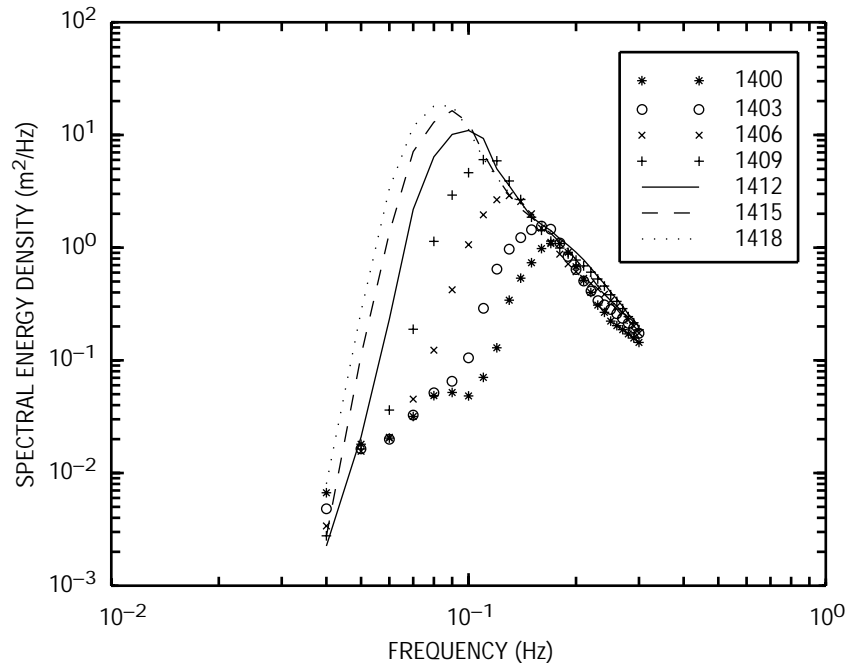


Fig. 19 — REF/DIF1 spectral density for 14 Mar 1997. Note changes in peak frequency from high to lower frequency due to wind-induced growth.

high-frequency waves is evident. The peak frequency evolves from high to lower frequency, showing a typical wave growth due to wind.

Unlike the STWAVE output, which included gridded fields of wave height, peak period, and mean wave direction, this implementation of REF/DIF1 provided only saved directional wave spectra at specified locations determined before generating the transformation coefficients. Figure 20 shows the directional distribution of the transformation coefficients, i.e., the output wave angle as a function of input frequency ( $x$  axis) and input angle ( $y$  axis). A general trend is evident as waves are bending toward shore normal (i.e., toward  $0^\circ$ ) as expected from the refraction process. It is interesting to note that the lower part of the angle distribution has more bending. An examination of the bathymetry contours confirms the fact that waves coming from the south side intersect the contours with sharper angles, thus resulting in more bending.

## 6.0 NAVY STANDARD SURF MODEL/SURF96 OVERVIEW

The Navy Standard Surf Model (NSSM) was developed (Earle 1988, 1989) because previous Navy surf forecasting techniques were largely manual, were based on methods dating to the 1950s, and did not adequately consider local shallow-water effects. NSSM is contained in the Geophysical Fleet Mission Program Library, the Tactical Environmental Support System, and the Mobile Oceanographic Support System. The NSSM has been used extensively by the Fleet and for several applications such as estimating climatological surf conditions at selected beaches for development of the Marine Corps' Advanced Amphibious Assault Vehicle (McDermid et al. 1997).

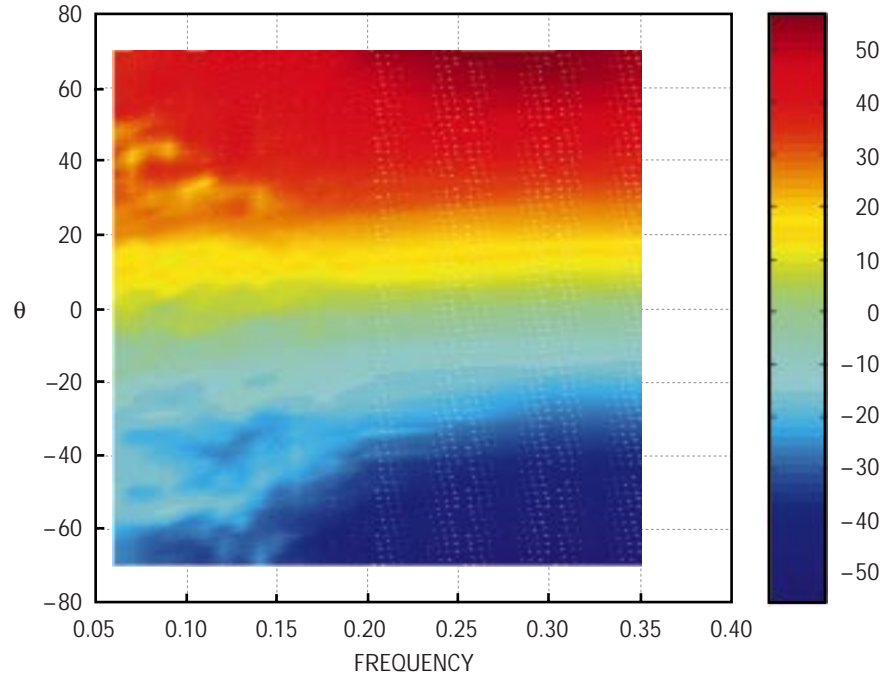


Fig. 20 — Directional distribution from REF/DIF1. Wave refraction is evident as waves at higher angles ( $\theta$ ) show more bending.

The NSSM is composed of two main modules, a wave refraction model and the surf model itself, SURF96. The most recent version of the surf model, SURF96, incorporates several theoretical and numerical improvements (Hsu et al. 1997, Miguez et al. in press) and was used for this work. SURF96 is an improved version of NSSM that is in the process of replacing NSSM Version 2.0 for operational Navy use. The surf model's strengths are rapid operation for field use and simulations, relatively simple operation and mathematical robustness for non-expert use, realistic depiction of breaking wave locations, and provision of detailed information (breaker heights, breaker types, longshore currents) across the surf zone. The model automatically provides parameters for planning amphibious operations as described in the *Joint Surf Manual* (COMNAVSURFPAC/COMNAVSURFLANT 1987).

In general terms, SURF96 numerically solves the steady-state energy balance equation considering dissipation of wave energy due to wave breaking

$$\frac{\partial(EC_g \cos \theta)}{\partial x} = -\langle \varepsilon_b \rangle, \quad (6)$$

where  $E$  is wave energy,  $C_g$  is wave group velocity,  $\theta$  is wave direction relative to a shore normal, and  $\langle \varepsilon_b \rangle$  is the average wave energy dissipation. The steady-state assumption is generally valid for the short times for waves to traverse the surf zone. Both  $C_g$  and  $\langle \varepsilon_b \rangle$  are functions of water depth at each point in the surf zone. The dissipation function  $\langle \varepsilon_b \rangle$  considers wave breaking as a function of water depth, wave period, and wave height, with wave heights determined from a depth-modified Rayleigh wave height distribution. Effects of breaker wave rollers are also considered in the formulation of  $\langle \varepsilon_b \rangle$ .

SURF96 is a one-dimensional (1D) parametric model largely based on breaking wave probability distribution concepts developed by Thornton and Guza (1983, 1986). The assumptions include:

- approximately straight and parallel bottom contours within the surf zone,
- a directional wave spectrum that is narrow-banded in frequency and direction,
- a Rayleigh wave height distribution, and
- linear wave theory.

The directional wave spectrum used for model initialization can be obtained from a wave model (WAM, STWAVE, REF/DIF1) or measurements. If an offshore directional wave spectrum is used, it must be properly refracted, shoaled, and diffracted to a starting depth that lies seaward of the breaker line. The directional wave energy distribution is reduced to three representative physical values: (1) the direction of the vertically averaged wave momentum flux, (2) the incident wave energy, and (3) the dominant wave frequency. The direction of the wave momentum flux is computed so that concentrating all wave energy in this direction yields the correct longshore momentum flux. The model incrementally calculates wave energy from which wave heights are determined along a transect normal to the beach to very near the beach and still water level. As waves move through the surf zone, the average rate of energy dissipation due to wave breaking and frictional dissipation balances the gradient of the shoreward energy flux. Longshore current calculations at each increment are based on longshore current theory using radiation stress (e.g., Longuet-Higgins 1970a,b). Current calculations include local wind stress effects. The longshore current module is being examined to provide improved performance for beaches with shallow offshore bars. Such a bar was not present for the Camp Lejeune simulations.

The percentage of breaking and broken waves across the surf zone is a model output. Surf-zone width is considered as the most seaward point where 10 percent of the waves are breaking or broken. Percentages of breaker type (spilling, plunging, or surging) are determined across the surf zone from the probability distribution of breaking waves using a widely accepted parameterization based on breaker height, breaker period, and bottom slope. Breaker height parameters specified in the *Joint Surf Manual* are determined for regions where breakers are largest. The Modified Surf Index (MSI) defined in the *Joint Surf Manual* is calculated automatically. The MSI determines whether or not particular types of conventional landing craft (not air-cushioned vehicles) can be used safely.

## 6.1 SURF96 Modeling Procedure for Camp Lejeune

### 6.1.1 SURF96 Input

The surf model uses four main inputs; wave spectra, winds, tides, and beach profile. SURF96 was run independently for Camp Lejeune using inputs from two models, STWAVE and REF/DIF1. The following section describes the inputs used in the Camp Lejeune SURF96 model runs.

**Wave Spectra.** Wave input clearly has a significant impact on surf model output (May and Mettlach 1998). Directional wave spectra for these simulations were provided from a pair of sources, STWAVE and REF/DIF1. While the same frequency bands were used in both models, STWAVE used 35 direction bands covering a half plane ( $180^\circ$ ) with a resolution of  $5^\circ$ . REF/DIF1 used 91 directions covering a half plane. The spectral energy from each is converted into a variance (in feet squared) inside the model so that the model is dealing with the same information no matter what the resolution of the input spectra.

**Winds.** A time series of winds was obtained from the Marine Corps Air Station in New River, NC. This was the closest hourly reporting station to Camp Lejeune, just a mile away. The wind speed and direction are input into the corresponding model run.

**Tides.** Tidal information was obtained from data generated by ADCIRC (see Sec. 4.2 for more information). The water elevations were read in, corresponding to each model run time, effectively raising or lowering the entire column of water in the beach profile.

**Beach Profiles.** Because wave refraction causes wave directions to be nearly perpendicular to the beach outside of the surf zone, SURF96 uses a 1D, perpendicular to the beach calculation traverse along which bathymetry is input. The beach orientation angle is important and must be specified. A beach profile file contains the distance offshore and the depth of the water at each point. The model uses these depths as it steps in toward the shore from a specified starting depth. A Navy SEAL beach survey collected for the Purple Star Exercise during 1997 was used as the beach profile in SURF96 model runs. Actual profiles for the time period of the model runs could be different but were not available. Appendix C shows the beach profile used for Camp Lejeune.

A method of approximating depth gradients involves use of an equilibrium beach profile (Dean 1977). In Dean's study, 502 beach profiles from the U.S. East Coast and the Gulf of Mexico were examined. The beach gradient depth profile is determined from the relation

$$D = Ax^{2/3}, \quad (7)$$

where  $D$  is the water depth,  $A$  is a coefficient related to sediment grain size, and  $x$  is the offshore distance from the beach. Figure 21 shows beach profiles for typical sediment types. These profiles are especially useful when existing profiles are missing data or as substitutes for beaches that are not surveyed prior to landing.

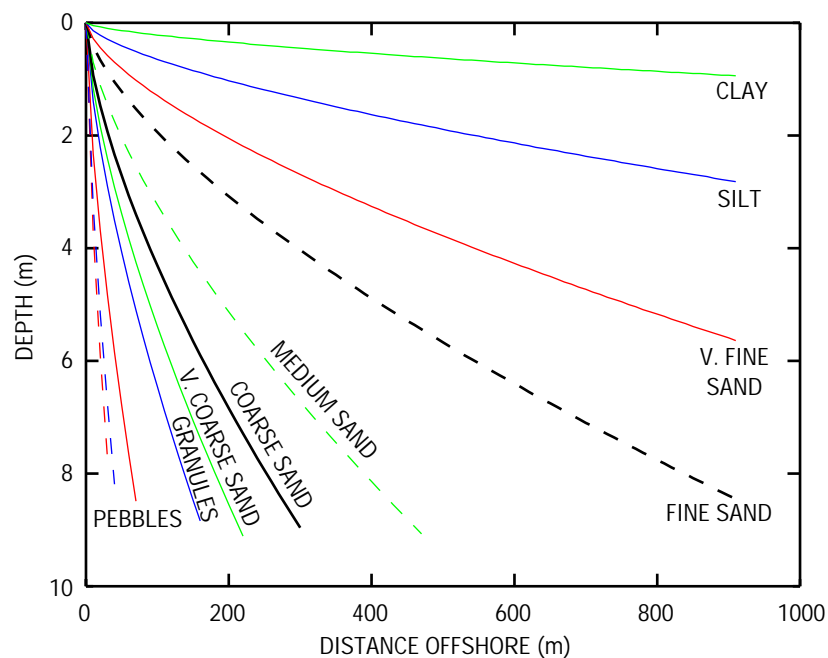


Fig. 21 — Equilibrium sediment beach profiles for sediments ranging from pebbles to fine sand to clay

**Input Options.** A namelist added to the SURF96 code allows for numerous options in each model run. The most useful options allow for multiple runs with output designated by date and specified type of spectral input. Rather than running just one time, a user specifies the beginning date and total number of runs and the program finds the correct input data for those dates including winds, tides, and wave spectra. Other, time-independent options can also be set, such as input spectra type (STWAVE or REF/DIF1), starting depth, size of step toward shore, and constant beach slope. Appendix D shows a truncated namelist used for these SURF96 model runs.

### 6.1.2 SURF96 Execution

Model execution is fairly straightforward once the starting time and number of time steps is set. The Camp Lejeune model runs began on 12 Mar at 00Z and proceeded at 3-hourly steps for 81 times through 22 Mar at 00Z. Once begun, the model denotes all output with the valid date. A detailed output of each step made by the surf model includes distance offshore, water depth, breaker height, percentage of breaking waves, wavelength, and current. Overall breaker period, angle, and type are also output, along with the MSI.

## 6.2 SURF96 Results

SURF96 hindcasts for the simulation period 12–22 Mar 1997 were performed using wave spectra from two sources, (1) REF/DIF1 and (2) STWAVE. Hourly wind speed and direction from the Marine Corps Air Station (34.7° N, 77.43° W) at New River, NC, were used. NORAPS winds were available; however, it was felt that observed winds would provide the most realistic input into SURF96. Because water elevations, including tides, affect surf, water elevations from ADCIRC were input into SURF96. The SURF96 code was adapted to accept wave spectra from REF/DIF1 and STWAVE.

Shallow-water wave spectra from STWAVE and REF/DIF1 hindcasts were saved for selected nearshore points. In this report, the directional spectra from both models at a 7-m depth along the beach survey line are used as input to SURF96. The 7-m location was selected so that only a small probability of depth-induced wave breaking occurred.

Figure 22 depicts SURF96 results for 15 Mar 03Z. The top panel shows the Navy SEAL beach team survey used as input to SURF96. The slope is rather steep from the coastline to approximately 250 m offshore (at a depth of 4 m) where the slope levels off. Figure 22b shows significant wave height along the shore-normal transect to 900 m offshore. The solid line depicts SURF96 results with input from STWAVE and the open circles represent results in which REF/DIF1 spectra were input. Figure 22c shows almost identical results of the percentage of breaking waves when comparing SURF96 output using inputs from REF/DIF1 and STWAVE. The surf-zone width (not shown) is defined as the offshore location where at least 10 percent of the waves break. This occurs at a distance of approximately 225 m. (Fig. 23 depicts the variation of surf-zone width with time.) The waves do not begin to break until water depths become less than 4 m because the input significant wave heights are between 2 and 3 m. Finally, Fig. 22d shows the longshore current variation with distance and model input into SURF96. The maximum longshore current occurs at a distance of 150 m offshore. Currents using STWAVE input show larger magnitudes than those using REF/DIF1 input in Fig. 22 because STWAVE surf-zone incident wave angles are slightly larger than those for REF/DIF1. Wave directions are incident at small angles from a perpendicular to the beach so that currents are sensitive to small changes in wave directions just outside of the surf zone. At various times, slightly different wave directions rather than different wave heights seem to account for current differences between the two model inputs.

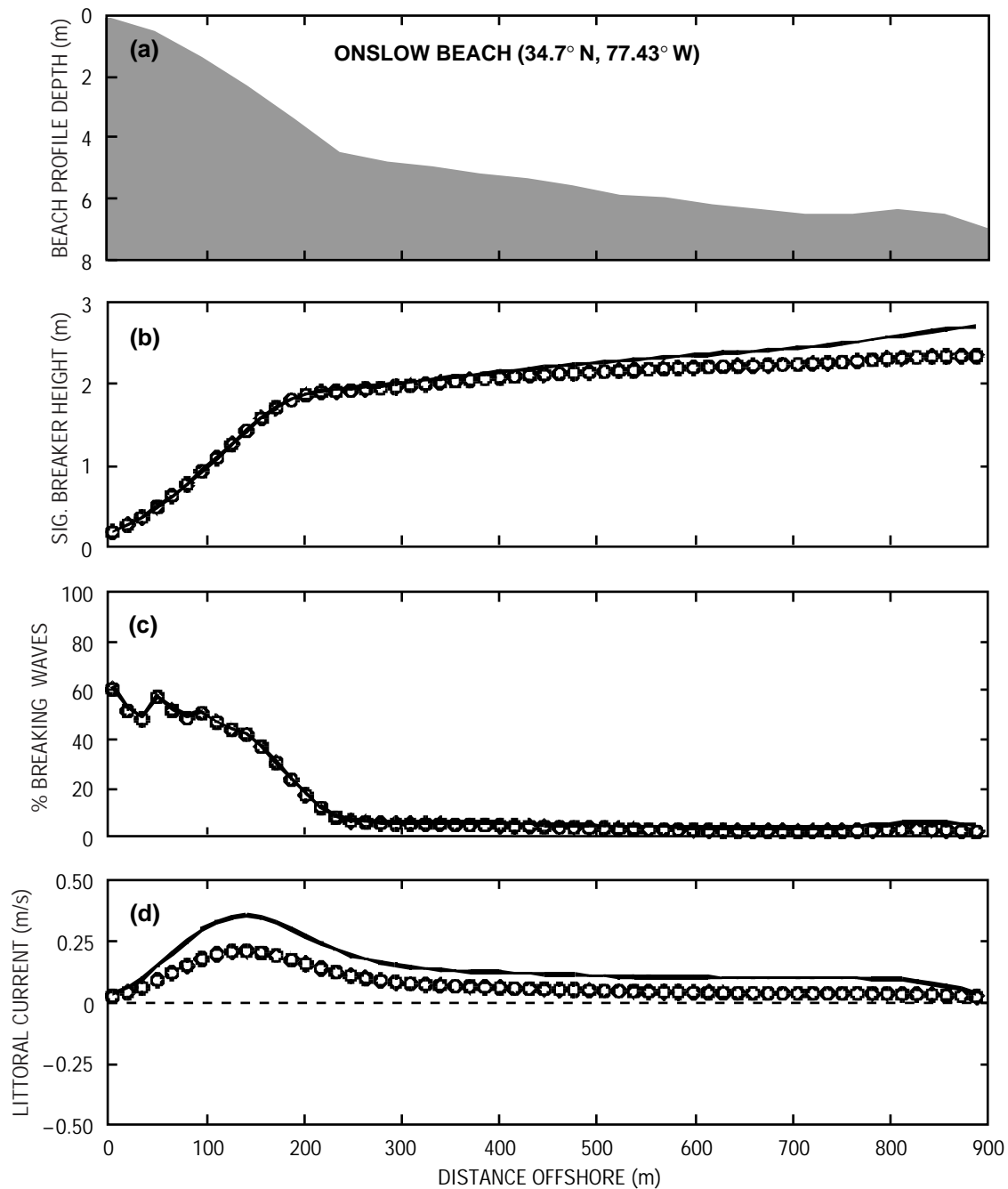


Fig. 22 — SURF96 output valid on 15 Mar 1997 03Z, (a) Navy SEAL team beach profile used in SURF96 calculations, (b) significant wave height (m) based on REF/DIF1 (circles) and STWAVE (solid) input, (c) percent breaking waves, and (d) longshore current (m/s)

Figure 23 presents time series of SURF96 output during 12–22 Mar 1997. The top panel depicts wind speed and direction provided from the Marine Corps Air Station. Wind speeds are highest on 15 Mar in advance of a strong cold front as wind directions are generally from the south. The wind gradually veers to the west and northwest as the cold front passes through the area and becomes southerly on 18 Mar. Late in the day on 19 Mar, the winds again shift to a direction from the north as yet another cold front passes through the area.

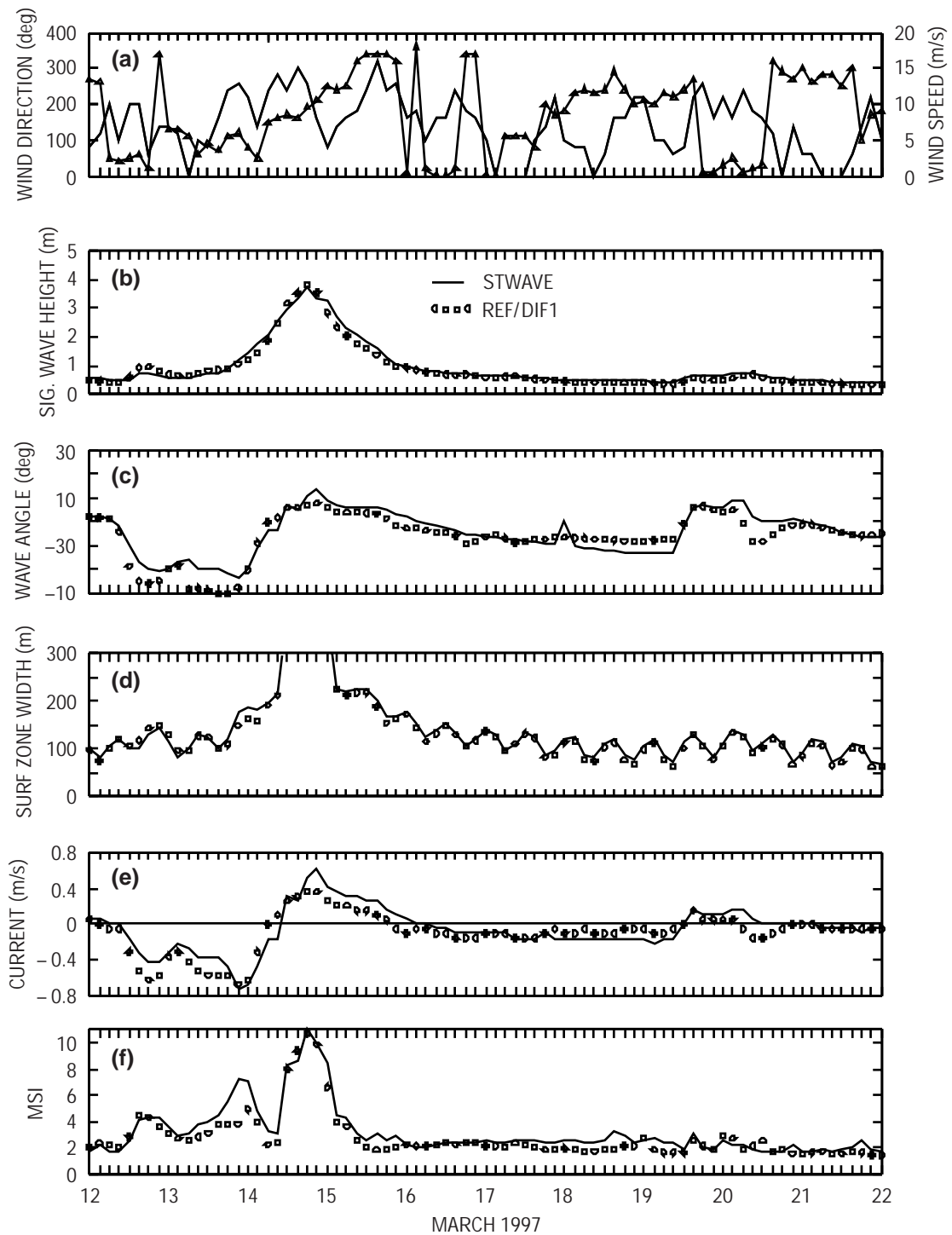


Fig. 23 — Time series of (a) wind direction (solid) and wind speed (dashed) near Onslow Beach, NC, (b) significant wave height (m) REF/DIF1 (circles) and STWAVE (solid) input, (c) wave angle (deg), (d) surf-zone width (m), (e) longshore current (m/s), and (f) MSI

The second panel depicts the significant wave height, which is an input parameter to the surf model. The solid line represents STWAVE, whereas the open circles denote REF/DIF1 output. Both models yield very similar results. The highest wave heights are associated with the major storm event occurring on 14 Mar.

The third panel shows the wave angle at 7-m depth where  $0^\circ$  represents waves moving perpendicular to the shoreline. A positive breaker angle is shown to be for breakers moving toward the right flank relative to a sight line perpendicular to the beach. Again, results from SURF96 with REF/DIF1 and STWAVE as inputs are similar. From 12 Mar 21Z to 13 Mar 18Z, REF/DIF1 shows a wave direction approximately  $10^\circ$  more negative than STWAVE. Some of this variation may be attributed to wind forcing, which is included in STWAVE, but is not for REF/DIF1. In addition, grid resolutions differ between STWAVE and REF/DIF1.

The fourth panel depicts the surf-zone width, which is defined as the offshore location where at least 10 percent of the waves are breaking. Throughout the 10-d hindcast period, surf-zone widths are generally between 60–200 m. The exception occurs during an 18-h period from 14 Mar 15Z to 15 Mar 03Z when the width reached 300 m, when a major storm event affected the area. The effects of tides are evident by the modulation in surf-zone width throughout the period. The fifth panel shows the longshore current with magnitude maxima near 0.8 m/s on 14 Mar. There is a change in current direction associated with changes in wind and wave directions relative to the beach.

The final panel shows the MSI, which is derived using the largest significant breaker height in the surf zone, maximum longshore current, breaker angle, wave period, and breaker type and based on the *Joint Surf Manual*. The significant breaker height in the surf zone is the average one-third highest breakers moving by the location. Depending on the amphibious landing craft, large values of MSI beyond a critical threshold value would deem a potential landing as unsafe. High values late on 14 Mar 97 would rule out use of most conventional amphibious landing craft.

## 7.0 IOP STOW 97 SUPPORT

The IOP Program was tasked by the Defense Advanced Research Projects Agency to provide an environmental representation of surf conditions for two landing beaches in support of the STOW 97 ACTD. The STOW 97 ACTD synthetic environment featured a  $500 \times 775$  km environmental data base (Lukes and Goodman 1998) integrating terrain and bathymetric data with time-varying representations of the atmosphere and ocean including the surf zone.

### 7.1 SURF96 Inputs

In this effort, SURF96 was coupled to NAVOCEANO's Persian Gulf WAM model to produce surf hindcasts for the landing beaches shown in Fig. 24 for the period 5–10 Dec 1996. In these simulations, wave refraction was not considered.

**Wave Spectra.** Directional wave spectra from NAVOCEANO's Persian Gulf ( $0.1^\circ$  resolution) located at  $29.4^\circ$  N,  $48.5^\circ$  E were used as input to both beach landing zones.

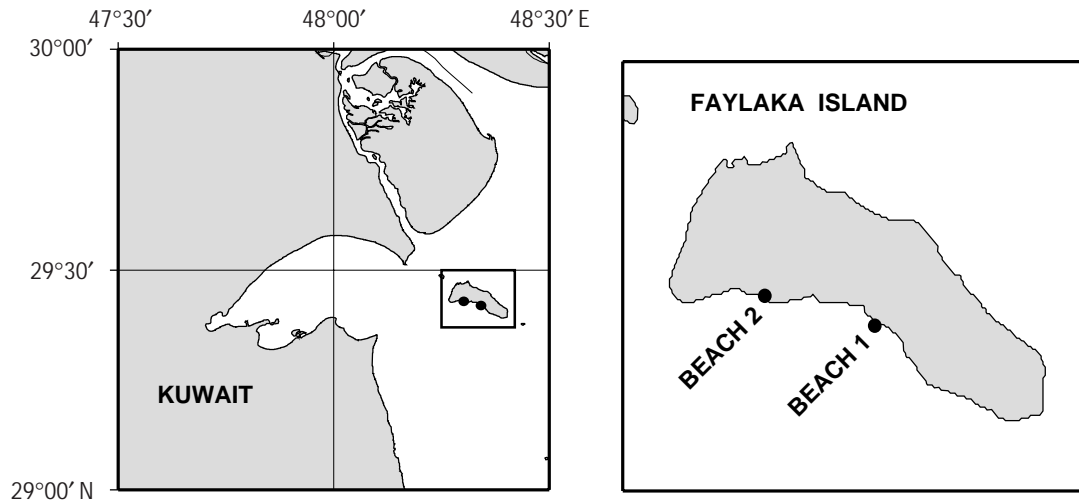


Fig. 24 — Location of landing beaches on Faylaka Island. SURF96 was run for these locations in support of the STOW 97 ACTD

**Beach Profiles.** Beach profiles for the primary and secondary beaches on Faylaka Island were derived from digitized National Imagery Mapping Agency Charts referenced to low water level.

**Tides.** The dominant semidiurnal tide in the Persian Gulf, M2, was computed using the QUODDY 3D finite-element hydrodynamic model developed at Dartmouth College (Lynch et al. 1996). ADCIRC was not set up for this quick response STOW 97 support. Model runs for this simulation were performed by NRL. The model domain encompasses the Persian Gulf, Gulf of Oman, and extends into the Arabian Sea. Forcing at the open ocean in the Arabian Sea is specified in the form of M2 tidal elevations derived from the Grenoble global tide model. The QUODDY model was exercised strictly in a barotropic mode, computing equilibrium M2 tidal amplitudes and phases. Tidal time series are reconstructed for the period 5 Dec 1996 00Z to 13 Dec 1996 23Z using standard tidal analysis techniques. Resolution of the finite-element mesh off the southern shores of Faylaka Island is approximately 3 km. Tidal elevations for the primary and secondary beach coordinates are approximated by tides computed at nearby nodal points, 29.424° N, 48.3° W and 29.419° N, 48.33° W, respectively. For computational purposes, the water depth at these points is set at a minimum of 5 m.

**Winds.** Indian Ocean NORAPS wind forcing inputs, which affect SURF96's calculations of the longshore current, were accessed through MEL.

## 7.2 IOP STOW 97 Results for Faylaka Island

Environmental inputs for both beach locations were very similar, only results for Faylaka Beach 1 (29.43° N, 48.3° E) will be discussed. Figure 25 depicts SURF96 hindcast results for the period 5–12 Dec 1996. The Indian Ocean NORAPS wind speed and direction are shown in Fig. 24 a,b. Winds were predominantly from the southeast from 5–10 Dec. A cold front passes through the region around 18Z on 10 Dec, causing winds to shift to the northwest. The MSI shown in Fig. 24c ranged from less than 1.0 to a maximum of 3.5 on 7 Dec 1996. Based on the MSI alone, landing craft should not face any serious threat from these surf conditions. Wave heights ranged from less than 0.3 m on 11–12 Dec and reached a peak of 1.3 m on 7 Dec at 12Z. The longshore current

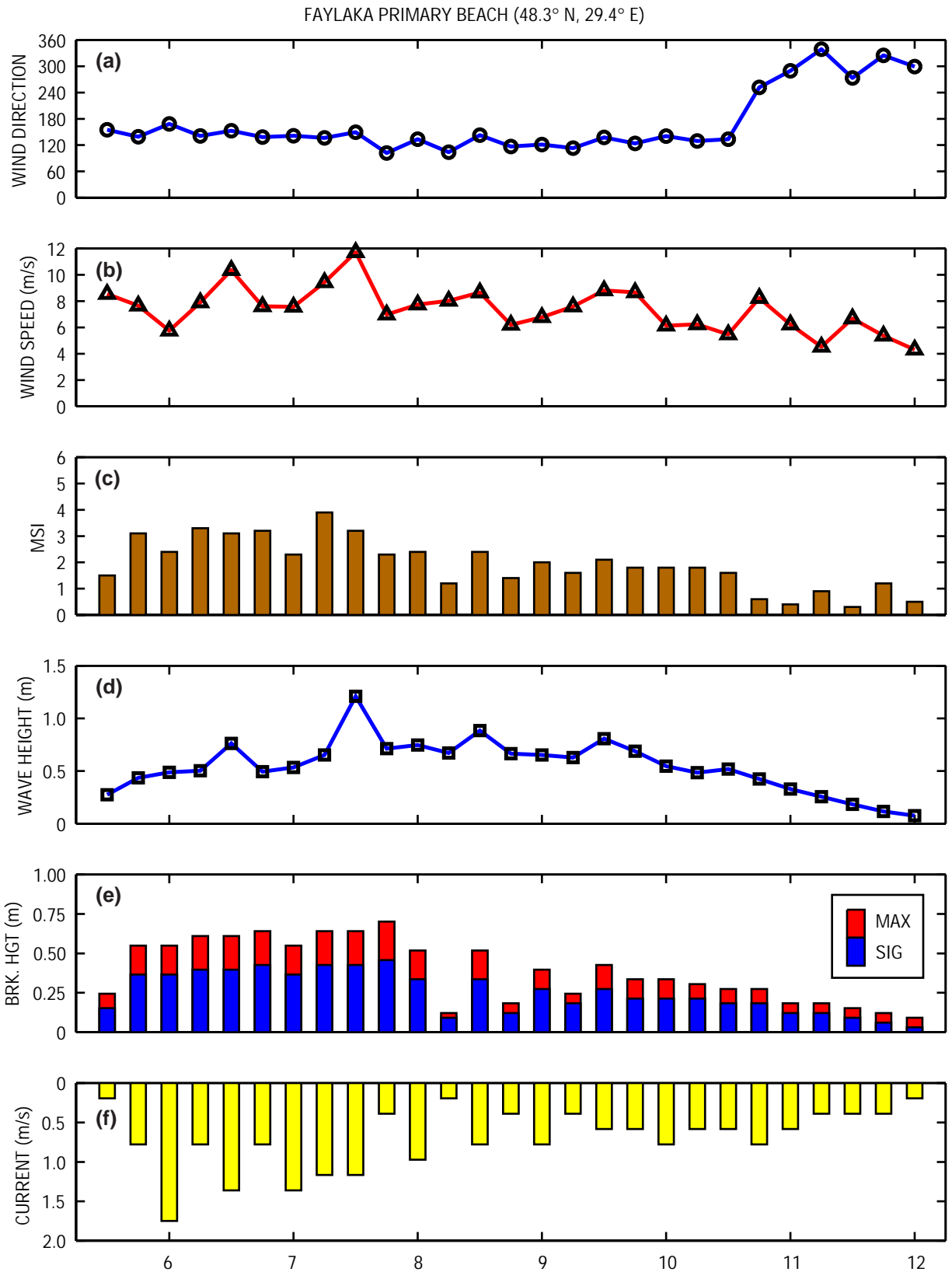


Fig. 25 — SURF96 hindcast results for the period 5–12 Dec 1996, (a) wind direction, (b) wind speed, (c) MSI, (d) wave height, (e) breaker height, and (f) longshore current

was directed toward the left flank (negative) throughout the period, with a maximum of  $-1.8$  m/s on 6 Dec 00Z.

## 8.0 IOP MODEL DATA AVAILABLE THROUGH MEL

Much of the data discussed for the IOP efforts at Camp Lejeune and Faylaka Island in this report are available on-line through the MEL (<http://mel.dms.o.mil>). MEL is an Internet-based information discovery and retrieval system that provides access to geographically distributed authoritative oceanographic, meteorological, terrain, and near-space data sets in standard interchange formats. A brief description of the IOP data sets in MEL follows.

### 8.1 Camp Lejeune (CLJ)

**NAVOCEANO WAM CLJ:** The North Carolina WAM model, run by NAVOCEANO, was forced with NORAPS CONUS wind stress fields. The model resolution is  $0.2^\circ$  and output is available on MEL for the period 12–22 Mar 1997 00Z at 12-h intervals. Output fields include significant wave height (meters), mean wave direction (degrees), mean wave period (seconds), swell wave height (meters), swell direction (degrees), and swell period (seconds).

**ADCIRC CLJ.** The ADCIRC model, run by the Coastal and Hydraulics Laboratory (CHL), was forced with NORAPS CONUS 10-m winds, surface pressures, and an M2 tide. The grid is unstructured with resolutions of 0.5 km and higher near the coastline. The model output is depth-averaged velocities and water elevations at 10-min intervals for 15 locations. The model was run for the time periods 12–23 Mar 1997 00Z.

**STWAVE CLJ Grid.** The STWAVE model was run by CHL and forced with CONUS NORAPS winds and wave spectra from NAVOCEANO's WAM model on the offshore boundary. Model output includes significant wave height (meters), mean wave direction (degrees), and peak wave period (seconds) on the  $201 \times 301$  STWAVE grid. The model was run for the period 12–23 Mar 1997 00Z at 3-h intervals.

**STWAVE CLJ Spectra.** STWAVE directional spectra (35 directions, 24 frequencies) saved at 15 locations at 3-h intervals from 12–23 Mar 1997 00Z.

**SURF96 CLJ Mar 97.** SURF96 model was run by NRL for a landing beach at Camp Lejeune, NC ( $34.557^\circ$  N,  $77.29^\circ$  W). This version of the model was forced with directional spectra from STWAVE. The surf information provided includes significant and maximum breaker height, dominant breaker period and direction, breaker type (spilling, plunging, surging), maximum longshore current, surf-zone width, and MSI. Model results are available from 13–22 Mar 1997 21Z.

**Onslow Bay, NC, Bathymetry.** This 3-arc-second resolution ( $\sim 100$  m) bathymetry is based on data from three sources, (1) NOS, (2) NRL survey data, and (3) NAVOCEANO STOIC data. The grid is dimensioned  $1800 \times 1200$ .

### 8.2 Faylaka Island, Kuwait

**Persian Gulf WAM.** This  $0.1^\circ$  resolution model was run by NAVOCEANO and is forced with Indian Ocean NORAPS winds. The model domain provided in MEL ranges from  $27.0$ – $31.0^\circ$  N,

47.5–53.5° E. Output fields include significant wave height, primary wave direction, mean wave period, swell height, swell direction, and swell period. Output from 00Z and 12Z runs with forecasts every 6 h out to 48 h are available for the period 21 Nov 1996 12Z–01 Jan 1997 00Z.

**Persian Gulf WAM Spectra.** Directional wave spectra (25 frequencies, 24 directions) from NAVOCEANO's Persian Gulf WAM model are saved for 36 locations in the Persian Gulf for the period 04–14 Dec 1996.

**SURF96 Beach 1.** SURF96 hindcasts for Faylaka Island Beach 1 (29.43° N, 48.302° E) are available for the period 05–12 Dec 1996 12Z. Data are available at 6-h intervals.

**SURF96 Beach 2.** SURF96 hindcasts for Faylaka Island Beach 2 (29.42° N, 48.342° E) are available for the period 05–12 Dec 1996 12Z. Data are available at 6-h intervals.

**Persian Gulf Bathymetry.** NAVOCEANO Digital Bathymetric Data Base Variable for the Persian Gulf. The data has a resolution of 0.03333° and covers the domain from 23.5–33.0° N, 45.0–60.0° E.

## 9.0 SUMMARY

This report documents the procedures used to create physically consistent integrated environmental representations of the surf zone using state-of-the-art, physics-based “off-the-shelf” wave, circulation, and surf models. To demonstrate the modeling procedures, a series of hindcasts were performed for the Onslow Bay, NC, area during the period 12–22 Mar 1997. In addition, recent efforts to support the STOW 97 effort are also discussed. Much of the data discussed in this report is available on-line from MEL (<http://mel.dmsomil>).

The deep-water WAM model shows very good agreement with available buoy and CMAN data. WAM directional wave spectra are independently fed into two shallow-water wave models, STWAVE and REF/DIF1. Model outputs from STWAVE and REF/DIF1 are remarkably similar. Outputs from STWAVE and REF/DIF1 drive a recent version of the NSSM, SURF96, to provide detailed information across the surf zone. Surf parameters of interest for simulations of military systems and amphibious operations are similar for inputs from both models. Use of water elevations, including tides, from ADCIRC illustrates effects that varying water elevations can have on the surf-zone width. Relatively high wave heights, large surf-zone widths, and high MSI values on 14 Mar show how combined use of these models can simulate conditions that could adversely affect use of military systems and amphibious operations.

Surf results based on wave inputs from two different models, STWAVE and REF/DIF1, were discussed. Although the Onslow Bay bathymetry is not very complicated, significant wave turning toward shore normal due to the refraction process is evident. SURF96 results indicate that both wave models handle the refraction and shoaling processes reasonably well. In this study, SURF96 does not appear to be very sensitive to the shape of the input wave spectrum. However, the selection of a shallow wave model for a particular area depends on wind, waves, climate, and the complexity of the bathymetry. For swell propagation in a more complicated bathymetry, REF/DIF1 may be best suited. However, STWAVE may be more appropriate if wind input is important and the offshore boundary is distant. In some cases, a nested STWAVE to REF/DIF1 model may be required. The following section discusses cautions and limitations associated with the models discussed in this report.

## 9.1 Cautions and Conclusions Related to Camp Lejeune Modeling Efforts

### 9.1.1 STWAVE, ADCIRC

The 2D steady-state, spectral wave transformation model STWAVE was used to transform WAM output into the surf zone. Use of a 2D ( $x$  and  $y$ ) model captures complex refraction patterns for regions of complex bathymetry, although the bathymetry at Camp Lejeune is fairly uncomplicated. Use of a spectral wave model preserves complex frequency and directional distributions in wave transformation. The depth-integrated, finite-element 2D circulation model ADCIRC was used to hindcast water surface elevation and currents through the nearshore driven by a tidal constituent data base and wind fields. The unstructured ADCIRC grid capability provides a flexible and efficient method to model circulation. The output wave spectra, water surface elevations, and currents from this study provide information required to construct realistic hydrodynamics for environmental simulations and site characterizations.

The procedures for applying STWAVE and ADCIRC are straightforward, but do require engineering judgement. The following cautions should be considered in applications:

- The STWAVE grid orientation should be aligned as closely as possible with the bathymetry contours. Nonalignment with the contours will lead to waves traveling offshore (relative to the grid) and errors in the model.
- Although STWAVE includes the dominant processes for most applications, the processes of reflection, diffraction from a structure, wave-current interaction, and triad interactions (growth of harmonics) are not included. These other processes are not expected to be important for the Camp Lejeune simulations.
- STWAVE is a time-independent model. For wave simulations where the wave field changes rapidly (faster than the time for a wave to propagate through the grid), a time-dependent model should be considered.
- The spectral input into STWAVE is assumed constant along the offshore boundary. Thus, if the wave field differs significantly across the boundary, the model requires some alteration.
- The ADCIRC grid boundaries should be far away from the region of interest.
- ADCIRC was run for this study with just one tidal constituent, so additional constituents should be added for more accuracy. Atmospheric pressure fields should be used as input if there are strong pressure variations throughout the grid. Short-wave stresses (e.g., calculated from STWAVE) that drive surf-zone current were also not included in this simulation.
- This study focused on Onslow Beach; thus, results in the inlets and on other parts of the grid, particularly velocity results, may not be accurate.

### 9.1.2 REF/DIF1

Similar considerations apply to REF/DIF1 so that some engineering judgement and model expertise is required to set up and run the model for new locations.

- Because waves approaching the beach at large angles must be treated carefully, multiple grids with varying geographic rotations may be needed.
- Sensitivity testing with different frequency and directional bandwidths is usually needed to optimize model application for a location.

- REF/DIF1 is a relatively time-consuming model to operate so that the described transfer function approach by which the model is operated ahead of time to develop wave transfer functions is the most efficient approach for simulations.
- The spectral input into REF/DIF1 is assumed constant along the offshore boundary. If the wave field differs significantly across the boundary, the model requires some alteration such as moving the offshore boundary to deeper water.
- Unlike STWAVE, REF/DIF1 does not have wind input on the seaward boundary.
- REF/DIF1 includes the effects of wave-current interaction, can handle complex bathymetry, and irregular coastlines.

### 9.1.3 SURF96

Similar considerations also apply to SURF96. In some ways, this model is more robust, partly because wave refraction causes wave directions to be closely perpendicular to the beach in most cases and because steady-state assumptions are valid for the short times that waves cross the surf zone. The following cautions apply.

- The depth profile along which depths are input should be generally perpendicular to the bottom contours and the beach itself. Different profiles and model runs should be employed at nearby locations if there is significant longshore depth variability.
- Because nearshore depths may change rapidly, best results are obtained using a recently measured profile such as that from a Navy SEAL Team survey.
- If an equilibrium depth profile based on sediment type is employed, effects of offshore shallow bars are not considered. Offshore bars may considerably affect surf conditions and the variability of surf conditions with time, particularly for locations with reasonable tide ranges.
- SURF96 should be operated with time-varying tides because tidal stages may significantly affect surf conditions.
- Longshore current variations across the surf zone are not accurately calculated by this model and other similar models when there are offshore shallow bars. This aspect is of present high research interest. However, most applications presently utilize the maximum current within the surf zone rather than current variations.

## 10.0 ACKNOWLEDGMENTS

This work was conducted under the sponsorship of the Ocean Executive Agent and the Defense Modeling and Simulation Office. Implementation of REF/DIF1 for Navy use was sponsored by the Space and Naval Warfare Systems Command (SPAWAR). The Office of Naval Research and SPAWAR sponsored NSSM improvements resulting in SURF96. The authors wish to thank Paul Farrar of NAVOCEANO for performing the WAM runs and providing WAM data, Cheryl Ann Blain (NRL) for running the QUODDY Model for the Gulf of Oman, Doug May (NRL) for providing bathymetry, John Breckenridge for running the TIN model and generating the high-resolution Onslow Bay bathymetry, Steve Foster (MSU-CAST) for making data available on MEL, CPL Barber for providing hourly wind observations from the Marine Corps Air Station at New River, NC, Cindy McClure and the Florida State University Meteorology Dept. for providing weather maps, and the National Data Buoy Center for providing buoy data. The authors acknowledge the office of the Chief of Engineers, U.S. Army Corps of Engineers, for authorizing publication of this report.

---

**11.0 REFERENCES**

- COMNAVSURFPAC/COMNAVSURFLANT, *Joint Surf Manual*, Instruction 3840.1B, 1987.
- Davis, J. E., "STWAVE Theory and Program Documentation," Chapter 8, in *Coastal Modeling System User's Manual*, Instructional Report CERC-91-1, Supplement 1, M. A. Cialone (ed.), U.S. Army Corps of Engineers Waterways Experiment Station, Vicksburg, MS, 1992.
- Dean, R. G., "Equilibrium Beach Profiles: U.S. Atlantic And Gulf Coasts," Ocean Engineering Technical Report 12, Department of Civil Engineering and College of Marine Studies, University of Delaware, Jan 1977.
- Earle, M. D., "Surf Forecasting Software Scientific Reference Manual," NORDA Technical Note 351, Naval Research Laboratory, Stennis Space Center, MS, 1989, 261 pp.
- Earle, M. D., "Surf Forecasting Software User's Manual," NORDA Technical Note 352, Naval Research Laboratory, Stennis Space Center, MS, 1988, 194 pp.
- ESRI, "ARC/INFO User's Guide, Surface Modeling with TIN™," Environmental Systems Research Institute, Inc., Redlands, CA, 1992.
- Hsu, Y. L., T. Mettlach, E. Kennelly, and M. Earle, "Interim Report on Validation of the Navy Standard Surf Model," NRL/MR/7322--97-8054, Naval Research Laboratory, Stennis Space Center, MS, 1997, 233 pp.
- Kaihatu, J. M., "Review and Verification of Numerical Wave Models for Near Coastal Areas – Part 1: Review of Mild-Slope Equation, Relevant Approximations and Technical Details of Numerical Wave Models," NRL/FR/7322--97-9669, Naval Research Laboratory, Stennis Space Center, MS, 1997, 27 pp.
- Kaihatu, J. M., W. E. Rogers, Y. L. Hsu, and W. C. O'Reilly, "Use of Phase-Resolving Numerical Wave Models in Coastal Areas," Proceedings of the 5th International Workshop on Wave Hindcasting and Forecasting, Melbourne, FL, 1998.
- Kirby, J. T., "A Note on Linear Surface Wave-Current Interaction," *Journal of Geophysical Research* **89**, 745–747 (1984).
- Kirby, J. T., "Higher-Order Approximations in the Parabolic Equation Method for Water Waves," *Journal of Geophysical Research* **91**, 933–952 (1986a).
- Kirby, J. T., "Rational Approximations in the Parabolic Equation Method for Water Waves," *Coastal Eng.* **10**, 355–376 (1986b).
- Kirby, J. T. and R. A. Dalrymple, "A Parabolic Equation for the Combined Refraction-Diffraction of Stokes Waves by Mildly Varying Topography," *J. Fluid Mech.* **136**, 543–566 (1983).
- Kirby, J. T. and R. A. Dalrymple, "Combined Refraction Diffraction Model REF/DIF1, Version 2.5, Documentation and User's Manual," Report 94-22, Center For Applied Coastal Research, University of Delaware, 1994.

- Komen, G. J., L. Cavaleri, M. Donelan, K. Hasselmann, S. Hasselmann, and P. A. E. M. Janssen, "Dynamics and Modelling of Ocean Waves," Cambridge University Press, Cambridge, U.K., 1994, 532 pp.
- Leenknecht, D. A. and W. W. Tanner, "Grid Generation and Data Analysis for Wave Transformation Models," Proceedings of the 4th Congress on Computing in Civil Engineering, Philadelphia, PA, 1997.
- Longuet-Higgins, M. S., "Longshore Currents Generated by Obliquely Incident Sea Waves 1," *J. Geo. Res.* **75**(33), 6778–6789 (1970a).
- Longuet-Higgins, M. S., "Longshore Currents Generated by Obliquely Incident Sea Waves 2," *J. Geo. Res.* **75**(33), 6790–6801 (1970b).
- Luetlich, R. A., J. J. Westerink, and N. Scheffner, "ADCIRC: An Advanced Three-Dimensional Circulation Model for Shelves, Coasts, and Estuaries, Report 1: Theory and Methodology of ADCIRC-2DDI and ADCIRC-3DL," Technical Report DRP-92-6, U.S. Army Corps of Engineers Waterways Experiment Station, Vicksburg, MS, 1992.
- Lukes, G. E. and G. Goodman, "Synthetic Environments and Lessons Learned from the STOW 97 ACTD," Proceedings of the Spring Simulation Interoperability Workshop, Orlando, FL, 1998.
- Lynch, D. R. and W. G. Gray, "A Wave Equation Model for Finite Element Tidal Computations," *Comp. Fluids* **7**, 207–228 (1979).
- Lynch, D. R., J. T. C. Ip, C. E. Naime, and F. E. Werner, "Comprehensive Coastal Circulation Model with Application to the Gulf of Maine," *Continental Shelf Res.* **16**(7), 875–906 (1996).
- May, D. and T. Mettlach, "Navy Surf Model: Comparative Performance of Alternative Initialization Parameter Sources," NRL/FR/7343--97-9670, Naval Research Laboratory, Stennis Space Center, MS, 1998, 41 pp.
- McDermid, J. G., M. D. Earle, D. C. Herringsaw, S. M. Mayfield, and C. R. Nichols, "METOC Conditions Affecting AAAV Ship-to-Objective Maneuver: A Detailed Analysis of Power Projection Points Sited Along Iranian and Korean Coasts," NRL/MR/7170--97-8060, Naval Research Laboratory, Stennis Space Center, MS, 1997.
- Migues, L., D. Osiecki, M. Earle, and T. Mettlach, "Software Design Document for the Oceanographic and Atmospheric Master Library, SURF 3.0 Forecasting Program," Neptune Sciences, Inc., report for the Naval Oceanographic Office (in press).
- Nichols, C. R. and M. D. Earle, "Use of a Coupled Wave Buoy-Surf Model System to Support Combined Joint Task Force Exercise-96/Purple Star," Report for Center for Tactical Oceanographic Warfare Support Program Office, Naval Research Laboratory, Stennis Space Center, MS, 1996.
- O'Reilly, W. C. and R. T. Guza, "A Comparison of Two Spectral Wave Models in the Southern California Bight," *Coastal Eng.* **19**, 263–282 (1993).
- Resio, D. T., "Shallow-Water Waves I: Theory," *Journal of Waterways, Ports, Coastal, and Ocean Engineering* **113**(3), 264–281 (1987).

- Resio, D. T., "Shallow-Water Waves II: Data Comparisons," *Journal of Waterways, Ports, Coastal, and Ocean Engineering* **114**(1), 50–65 (1988a).
- Resio, D. T., "A Steady-State Wave Model for Coastal Applications," Proceedings of the 21st Coastal Engineering Conference, ASCE, 929–940, 1988b.
- Thornton, E. B. and R. T. Guza, "Transformation of Wave Height Distributions," *J. Geo. Res.* **88**(C10), 5925–5938 (1983).
- Thornton, E. B. and R. T. Guza, "Surf Zone Longshore Currents and Random Waves: Field Data and Models," *J. Phys. Oceanogr.* **16**, 1165–1178 (1986).
- Turner, P. J. and A. M. Baptista, "ACE/Gredit User's Manual: Software for Semi-Automatic Generation of Two-Dimensional Finite Element Grids," Center for Coastal and Land Margin Research, Oregon Graduate Institute of Science and Technology, Beaverton, OR, 1993.
- WAMDI Group, "The WAM Model – A Third-Generation Ocean Wave Prediction Model," *J. Phys. Ocean.* **18**, 1775–1810 (1988).
- Westerink, J. J., R. A. Luettich, and N. Sheffner, "ADCIRC: An Advanced Three-Dimensional Circulation Model for Shelves, Coasts, and Estuaries, Report 3: Development of a Tidal Constituent Data Base for the Western Atlantic and Gulf of Mexico," Technical Report DRP-92-6, U.S. Army Corps of Engineers Waterways Experiment Station, Vicksburg, MS, 1993.
- Westerink, J. J., C. A. Blain, R. A. Luettich, and N. Sheffner, "ADCIRC: An Advanced Three-Dimensional Circulation Model for Shelves, Coasts, and Estuaries, Report 2: Users's Manual For ADCIRC-2DDI," Technical Report DRP-92-6, U.S. Army Corps of Engineers Waterways Experiment Station, Vicksburg, MS, 1994.
- Wittmann, P. A. and P. D. Farrar, "Global, Regional, and Coastal Wave Prediction," *MTS Journal* **31**, 76–82 (1997).

## Appendix A

### SAMPLE STWAVE OPTIONS FILE

201 301 25 35 250.000 1 0 14  
0.0333 0.0367 0.0403 0.0444 0.0488 0.0537 0.0591 0.0650 0.0715 0.0786  
0.0865 0.0951 0.1046 0.1151 0.1266 0.1392 0.1532 0.1685 0.1853 0.2039  
0.2243 0.2467 0.2713 0.2985 0.3283  
90, 136  
90, 137  
95, 38  
100, 139  
100, 140  
119, 246  
100, 146  
115, 41  
115, 42  
109, 243  
105, 39  
105, 41  
105, 36  
105, 37

## Appendix B

### SAMPLE ADCIRC OPTIONS FILE (PARTIAL LISTING)

```
model_grid8k      ! 30 CHARACTER ALPHANUM RUN DESCRIPTION
v29.06 iterative  ! 20 CHARACTER ALPNUMERIC RUN IDENTIFICATION
1                ! NFOVER - NONFATAL ERROR OVERRIDE OPTION
0                ! NABOUT - ABBREVIATED OUTPUT OPTION PARAMETER
1                ! NSCREEN - UNIT 6 OUTPUT OPTION PARAMETER
67              ! IHOT - HOT START PARAMETER
2                ! ICS - COORDINATE SYSTEM SELECTION PARAMETER
0 ! IM - MODEL TYPE (0 INDICATES STANDARD DEPTH INTEGRATED MODEL)
2 ! NOLIBF - BOTTOM FRICTION TERM SELECTION PARAMETER
2 ! NOLIFA - FINITE AMPLITUDE TERM SELECTION PARAMETER
0 ! NOLICA - SPATIAL DERIVATIVE PORTION OF CONV. TERM SELECTION PARAMETER
0 ! NOLICAT - TIME DERIVATIVE PORTION OF CONVECTIVE TERM SELECTION PARAMETER
0 ! NWP - VARIABLE BOTTOM FRICTION AND LATERAL VISCOSITY OPTION PARAMETER
1 ! NCOR - VARIABLE CORIOLIS IN SPACE OPTION PARAMETER
0 ! NTIP - TIDAL POTENTIAL OPTION PARAMETER
3 ! NWS - WIND STRESS AND BAROMETRIC PRESSURE OPTION PARAMETER
1                ! NRAMP - RAMP FUNCTION OPTION
9.81            ! G - ACCELERATION DUE TO GRAVITY - DETERMINES UNITS
0.002           ! TAU0 - WEIGHTING FACTOR IN GWCE
4.0             ! DT - TIME STEP (IN SECONDS)
0.0             ! STATIM - STARTING TIME (IN DAYS)
0.0             ! REFTIM - REFERENCE TIME (IN DAYS)
97 03 10 00 0 0 ! IREFYR,IREFMO,IREFDAY,IREFHR,IREFMIN,REFSEC
21 21 40. -80. 0.5 0.5 21600 ! NWLAT,NWLON,WLATMAX,WLONMIN,WLATINC,WLONINC,WTIMINCR
13.0            ! RNDAY - TOTAL LENGTH OF SIMULATION (IN DAYS)
2.0             ! DRAMP - DURATION OF RAMP FUNCTION (IN DAYS)
0.35 0.30 0.35 ! TIME WEIGHTING FACTORS FOR THE GWCE EQUATION
0.02 10 10 0.02 ! H0 - MINIMUM CUTOFF DEPTH
-76.0 33.0      ! SLAM0,SFEA0 - CENTER OF CPP PROJECTION IN DEGREES LONG/LAT
0.0025 1.0 10. 0.3333 ! FFACTOR - BOTTOM FRICTION COEFFICIENT
2.0            ! ESL - LATERAL EDDY VISCOSITY COEFFICIENT; IGNORED IF NWP =1
0.0           ! CORI - CORIOLIS PARAMETER - IGNORED IF NCOR = 1
0            ! NUMBER OF TIDAL POTENTIAL CONSTITUENTS BEING FORCED
1            ! NBFR - TOTAL NUMBER OF FORCING FREQUENCIES ON OPEN BOUNDARIES
M2
0.000140518902509 0.4671 336.241 ! NODAL FACTOR 1.038*0.45 = 0.4671
M2            ! ALPHANUMERIC DESCRIPTION OF OPEN BOUNDARY FORCING DATA SET WHICH
FOLLOWS
.7163 354.53 57 0
.7163 354.53 57 0
```

```

.7163 354.53 57 0
.7163 354.53 57 0
.
.
.5730 356.40 30695 0
.5730 356.40 30695 0
100.0 ! ANGINN : INNER ANGLE THRESHOLD
1 2.0 13.0 150 ! NOUTE,TOUTSE,TOUTFE,NSPOOLE:ELEV STATION OUTPUT INFO (UNIT 61)
15 ! TOTAL NUMBER OF ELEVATION RECORDING STATIONS
-76.6700 34.7167 ! Duke Marine Lab (Station 6)
-76.7367 34.7200 ! Atlantic Beach Bridge (Station 9)
-76.6200 34.7083 ! Lenoxville Point (Station 11)
-76.7683 34.7000 ! Coral Bay (Station 13)
-76.6817 34.6983 ! Fort Macon (Station 16)
-76.7117 34.6933 ! Atlantic Beach (Station 17)
-76.5383 34.6133 ! Cape Lookout (Station 18)
-77.117340 34.641735 ! Points across Bogue Inlet
-77.266667 34.550000 ! new station 1
-77.250000 34.533333 ! new station 2
-77.233333 34.516667 ! new station 3
-77.166667 34.200000 ! new station 4
-77.000000 34.200000 ! new station 5
-77.339029 34.528202 ! New River Inlet A
-77.337728 34.528129 ! New River Inlet B
1 2.0 13.0 150 ! NOUTE,TOUTSE,TOUTFE,NSPOOLE:VEL STATION OUTPUT INFO (UNIT 62)
15 ! TOTAL NUMBER OF ELEVATION RECORDING STATIONS
-76.6700 34.7167 ! Duke Marine Lab (Station 6)
-76.7367 34.7200 ! Atlantic Beach Bridge (Station 9)
-76.6200 34.7083 ! Lenoxville Point (Station 11)
-76.7683 34.7000 ! Coral Bay (Station 13)
-76.6817 34.6983 ! Fort Macon (Station 16)
-76.7117 34.6933 ! Atlantic Beach (Station 17)
-76.5383 34.6133 ! Cape Lookout (Station 18)
-77.117340 34.641735 ! Points across Bogue Inlet
-77.266667 34.550000 ! new station 1
-77.250000 34.533333 ! new station 2
-77.233333 34.516667 ! new station 3
-77.166667 34.200000 ! new station 4
-77.000000 34.200000 ! new station 5
-77.339029 34.528202 ! New River Inlet A
-77.337728 34.528129 ! New River Inlet B
1 2. 13. 1800 ! NOUTGE,TOUTSGE,TOUTFGE,NSPOOLGE : GLOBAL ELEV OUTPUT (UNIT 63)
1 2. 13. 1800 ! NOUTGV,TOUTSGV,TOUTFGV,NSPOOLGV : GLOBAL VEL OUTPUT (UNIT 64)
1 2. 13. 1800 ! NOUTGW,TOUTSGW,TOUTFGW,NSPOOLGW: GLOBAL OUTPUT INFO (UNIT 74)
0 ! NHARFR - # FREQS IN HAR ANAL
6.0 8.0 150 0.000000 ! THAS, THAF, NHAINC,FMV
1 1 1 1 ! NHASE,NHASV,NHAGE,NHAGV
1 5400 ! NHSTAR,NHSINC
1 0 1e-5 25 ! ITITER,ISLDIA,CONVCR,ITMAX

```

## Appendix C

### CAMP LEJEUNE BEACH PROFILE

Camp Lejeune Beach Profile, 77.289284W, 34.557247N

INDEX	OFFSHORE DISTANCE (m)	WATER DEPTH (m)			
-4	-189.96	-3.34	43	1995.42	10.11
-3	-142.02	-2.25	44	2042.53	10.02
-2	-94.91	-1.30	45	2089.98	9.72
-1	-47.11	-0.51	46	2137.93	9.17
1	0.00	0.00	47	2185.38	8.81
2	47.11	0.51	48	2232.84	8.85
3	94.91	1.30	49	2279.94	8.91
4	142.02	2.25	50	2327.40	8.82
5	189.96	3.34	51	2375.34	8.71
6	237.07	4.41	52	2422.80	8.77
7	284.87	4.76	53	2469.90	8.78
8	332.33	4.91	54	2517.71	8.78
9	379.43	5.11	55	2565.51	8.88
10	427.72	5.31	56	2613.11	9.01
11	475.18	5.55	57	2660.56	9.14
12	522.63	5.80	58	2707.67	9.28
13	569.39	5.94	59	2755.47	9.85
14	617.34	6.15	60	2802.24	10.51
15	665.14	6.34	61	2850.18	10.95
16	712.25	6.43	62	2897.98	11.18
17	759.70	6.43	63	2945.09	11.38
18	806.81	6.32	64	2992.54	11.31
19	855.10	6.49	65	3039.65	11.05
20	902.20	6.91	66	3087.94	10.78
21	950.01	7.18	67	3135.05	10.56
22	997.46	7.37	68	3182.85	10.37
23	1045.40	7.38	69	3230.30	10.17
30	1377.73	7.47	70	3278.25	10.04
31	1425.53	7.55	71	3325.70	10.01
32	1473.13	7.56	72	3372.81	10.06
33	1520.59	7.96	73	3420.26	10.13
34	1567.35	8.68	74	3467.72	10.21
35	1614.80	9.25	75	3515.66	10.27
36	1662.26	9.69	76	3563.12	10.30
37	1709.86	10.03	77	3610.22	10.36
38	1757.66	9.98	78	3658.03	10.54
39	1804.77	9.97			
40	1852.22	10.11			
41	1899.68	10.21			
42	1947.62	10.21			

## Appendix D

### SAMPLE SURF96 NAMELIST

```
&input1
  gt_frq  =8
  roller  =.false.
  M_type  =4
  lin_stress=.false.
  soln    ='analytic'
&end
&input2
  iyear   =97
  imonth  =3
  iday    =12
  ihour   =00
  imin    =00
  dtfore  =3
  numtimes =80
  windfile ='mcas.dat'
  tidefile ='cltidejms.dat'
  yrefrac  ='N'
  ystr     ='Y'
  self_st  ='N'
  fracname ='straight.frc'
  lndname  ='TEST'
  ydepth   ='Y'
  slope    =0.01
  ydetail  ='Y'
  dstart   =23.0
  wavdep   =0.0
  bchname  ='lejeunerefdif'
&end
'end'
```

## Appendix E

### SAMPLE SURF96 OUTPUT FILE (PARTIAL LISTING)

Internal grid spacing = 2.0 ft.  
 Significant Wave Height from WAM Offshore value = 1.95ft.  
 OPTION 1: DELILAH Spectra used  
 OPTION 2: NO roller term.  
 OPTION 3: Breaking wave probability function:  $pb(H) = W(H)*p(H)$  where  
 $W(H) = (Hrms/(\gamma*h))^4 * \{1 - \exp(-H/(\gamma*h))^2\}$   
 OPTION 4: Linear Bottom Stress Function  
 used to calculate longshore current (Krauss Method)  
 Significant Wave Height Offshore = 1.95 ft  
 Radiation Stress Significant Wave Height (energy toward shore) = 1.95 ft  
 Radiation Stress Peak Frequency = 0.1266 Hz  
 Radiation Stress Zero-Crossing Frequency = 0.1706 Hz  
 Radiation Stress Peak Period = 7.8999 sec

\*\*\*\*\* SURF FORECAST \*\*\*\*\*

Date and time of forecast: 97/03/13 0000

\*\*\*\*\* Detailed Surf Output Follows \*\*\*\*\*

Index	Distance Offshore (ft)	Water Depth (ft)	Significant Breaker Ht. (ft)	Maximum Breaker Ht. (ft)	Percent Breaking Waves	Wave Length (ft)	Littoral Current (kts)
1	2959.0	22.3	2.0	3.0	0.0	196.7	0.04
2	2954.0	22.3	2.0	3.0	0.0	195.6	0.04
3	2949.0	22.3	2.0	3.0	0.0	195.6	0.04
4	2944.0	22.2	2.0	3.0	0.0	195.6	0.04
5	2939.0	22.2	2.0	3.0	0.0	195.6	0.04
6	2934.0	22.1	2.0	3.0	0.0	195.6	0.04
7	2929.0	22.1	2.0	3.0	0.0	195.6	0.04
8	2924.0	22.0	2.0	3.0	0.0	194.6	0.04
9	2919.0	22.0	2.0	3.0	0.0	194.6	0.04
10	2914.0	21.9	2.0	3.0	0.0	194.6	0.04
.	.	.	.	.	.	.	.
.	.	.	.	.	.	.	.
.	.	.	.	.	.	.	.
556	184.0	1.8	1.1	1.4	48.7	60.6	0.49
557	179.0	1.8	1.0	1.4	49.8	59.5	0.48
558	174.0	1.7	1.0	1.3	50.9	57.8	0.46
559	169.0	1.6	1.0	1.2	52.1	56.6	0.44
560	164.0	1.5	0.9	1.2	53.3	54.8	0.42
561	159.0	1.4	0.9	1.1	54.6	53.6	0.40
562	154.0	1.4	0.8	1.1	55.5	51.8	0.38
563	149.0	1.3	0.8	1.0	51.9	50.9	0.35
564	144.0	1.2	0.7	1.0	48.9	49.6	0.33
565	139.0	1.2	0.7	0.9	47.2	48.0	0.30

566	134.0	1.1	0.7	0.9	46.3	47.4	0.28
567	129.0	1.1	0.6	0.8	46.0	46.5	0.26
568	124.0	1.0	0.6	0.8	46.1	45.0	0.24
569	119.0	1.0	0.6	0.8	46.5	44.1	0.22

\*\*\*\*\* Input Summary \*\*\*\*\*

SURF96 ver 1.1 (24 FEBRUARY 1997)  
 Session logged to file 97031300.out  
 date & time = 97/03/13 0000  
 Landing zone name = CLJ  
 Sight line, Interval, Starting depth = 180.0 deg. true, 5.0 ft, 23.0 ft.  
 Depth profile file = lejeune.dep  
 Wind speed and direction = 7.0 kts, 130.0 deg. true.  
 Tide level = -0.33 ft. Detailed output obtained.  
 \*\*\*\*\* Coded Surf Forecast Follows \*\*\*\*\*

Landing zone: TEST  
 Depth profile: lejeune.dep  
 Date and time of forecast: 97/03/13 0000  
 Significant breaker height alfa = 2.4 ft.  
 Maximum breaker height bravo = 3.6 ft.  
 Dominant breaker period charlie = 7.9 sec.  
 Dominant breaker type delta = spilling surf  
 (97% spilling, 3% plunging, 0% surging)  
 Breaker angle (toward right flank) echo = 19.4 deg.  
 Littoral current (toward right flank) foxtrot = 0.6 kts.  
 Number of surf lines golf1 = 5.5  
 Surf zone width golf2 = 384.9 ft.  
 Wind speed hotel1 = 7. kts.  
 Wind direction hotel2 = 130. deg. true  
 Modified surf index = 3.6